DETECTION OF LAUREL WILT DISEASE FOR AVOCADO TREES USING MULTISPECTRAL IMAGING AND A SPECTRODIOMETER

By

JAAFAR ABDULRIDHA

A DISSERTATION PRESENTED TO THE GRADUATE SCHOOL
OF THE UNIVERSITY OF FLORIDA IN PARTIAL FULFILLMENT
OF THE REQUIREMENTS FOR THE DEGREE OF
DOCTOR OF PHILOSOPHY

UNIVERSITY OF FLORIDA

2016

To Spirit of my father, mother and to my lovely wife and my daughter

ACKNOWLEDGMENTS

I would like to express my thanks, gratitude, and appreciation to my chair Dr. Reza Ehsani, professor of Agricultural and Biological Engineering at the Citrus Research and Education Center (CREC), University of Florida (UF) for his consistent help and support, enabling me to complete my doctoral requirements at UF. He was advisor, guide, and a great reference for me. I am greatly indebted to my supervisory committee: Dr. Amr Abd-Elrahman, associate professor of Geomatics at UF, Dr. John Schueller, professor of Mechanical and Aerospace Engineering at UF, Dr. Larry Duncan, professor of Nematology at Citrus Research and Education Center (CREC), University of Florida (UF), Dr. Ray Bucklin, professor of Agriculture and Biological Engineering. Their concepts, understanding, and ideas have helped me to overcome all the obstacles that I faced. Dr. Randy Ploetz and Joshua Konkan, at TREC, UF helped by preparing greenhouse samples at Homestead. I would like to thank Dr. Ana de Castro and Sherrie Buchanon for their suggestions and guidance in my data analysis, also Dr. Chris Martinez, assistant professor of Agriculture and Biological Engineering, UF, for expediting my acceptance at UF for the first time. I am also thankful to Robin Snyder, ABE, Jennifer Dawson and Kathy Snyder at CREC library in technical and administrative matters.

Special thanks to my wife Wijdan, who sacrificed so much for me. May Allah bless her. I would like to thank my sweetheart Fatimah, my daughter, for her patience because I was always busy with my studies, and I did not spend enough time with her. I would like to thank the Iraqi Ministry of Higher Education and Research for financial support through 5 years of my study. I appreciate everybody who advised and guided me, my family (Mother, Uncle Juhi, brother and sisters) and every member at CREC UF. I won’t forget to thank my neighbor Kate Lehne.

TABLE OF CONTENTS

LIST OF TABLES

LIST OF FIGURES

Abstract of Dissertation Presented to the Graduate School
of the University of Florida in Partial Fulfillment of the
Requirements for the Degree of Doctor of Philosophy

DETECTION OF LAUREL WILT DISEASE FOR AVOCADO TREES USING MULTISPECTRAL IMAGING AND A SPECTRODIOMETER

By

Jaafar Abdulridha

December 2016

Chair: Reza Ehsani
Major: Agricultural and Biological Engineering

Early detection of plant disease is critical for managing the disease. Many of these diseases have similar symptoms, making it difficult to expect which infection might occur. The right steps to discover the stress factor and disease spread are unknown. Recently, Florida avocado industry has started facing a devastating disease called laurel wilt; this disease has symptoms similar to nutrient deficiency and other diseases. Currently, aerial scouting by helicopter in combination with ground scouting is the common method to inspect laurel wilt disease. This is a time consuming and expensive method to manage huge areas prone to error because it depends on visual observation. The main objective of this study is to discriminate laurel wilt infected avocado trees from other diseases and nutrient deficiency such as Phytophthora root rot, salinity damage, and Fe and N deficiency. The dissertation includes description of laurel wilt and the effect of this disease on productivity in avocado crops in Florida, and the advantage of remote sensing technique and spectrodiometer band selection. It also includes review of some diseases and nutrient deficiencies with same symptoms, making it difficult to distinguish laurel wilt from other less risky factors.

In order to evaluate and select the best bands that could discriminate Lw from other factors, handheld spectrodiometer (SVC HR-1024) (Spectra Vista Cooperation, NY, USA) (350-2500 nm) was utilized to collect spectral data; the reflectance data were averaged each 10 and 40 nm bands to reduce band r; also in that range unexpansive filters are available. From the result, there are several bands that could distinguish stress factor from healthy, especially in green, red, and near infrared (400-970 nm), therefore distinguishing between; best bands were selected and highest weight value (100%) healthy, laurel wilt, salinity damage, and phytophthora root rot using neural network multilayer perceptron (MLP) and the best bands were selected in average 10 and 40 were between 700 to 750 nm and 800 to 862 nm, respectively. Stepwise discernment analysis (STEPDISC) and radial basis functions (RBF) were used but they were less accurate than MLP. Decision tree (DT) and K-nearest neighbor (KNN) method were used and showed the ability to distinguish healthy from other stress factors, but it have less accuracy than the MLP method. Therefore, we depend on MLP result to select 6 bands for Tetra cam, Canon cam, the most important bands were in red edge and near infrared. MLP method was run in all analysis; it was the best method of all. Best bands were selected and applied in image processing technique using two different types of cameras Canon (CanonSX260 NDVI, Canon U.S.A., Inc. Melville, NY, USA), Tetra cam 6 bands (Tetra cam, Inc., CA, USA) to classify Lw from healthy and other factors. Filter was built according to bands chosen for Tetra cam 6 bands (G: 580 nm; R650, Redge740 nm, Redge750 nm, NIR760, NIR850 nm), and Canon camera with 3 bands (B: 390-520 nm; green, G: 470-570 nm; red-edge, R mod: 670-750 nm) to distinguish healthy plant from non-healthy such as laurel wilt (Lw), Phytophthora root rot (Prr), Fe and N deficiency. Two classification methods were utilized: neural network multilayer perceptron (MLP), and K-nearest neighbor. Image processing was applied for polygon region of interest (PROI) and overall region

of interest (OVROI). According to the results, MLP was the highest value for all treatments, and Tetra cam 6 bands - overall region of interest obtained the best result in all classifications. From the results, we could use these filters in order to distinguish healthy from other stress factors. It is possible to utilize inexpensive remote sensing technique to cover wide area with low cost in time. These images were processed in ENVI 4.5 (ITT Visual Information Solutions, Boulder, Colorado). Various vegetation indices were applied. Results showed that multispectral imaging has the potential to discriminate Lw from healthy and other stress factors. In this dissertation, the related literature on application of remote sensing in agriculture is studied. The application of remote sensing and the effect of stress plant is reviewed. The most important objective in this study is focused on disease detection to detect Lw and separate from healthy avocado trees, Phytophthora disease, salinity damage, and the separation of Lw and nutrient deficiency (N, Fe) followed by discussion of current operational developments. First, the fundamentals of remote detecting are introduced, followed by an explanation of the corporate application of remotely sensed data in agriculture field, and the effect of the diseases on crop growth parameters. The discussion continues with a brief introduction of various crops and various pathogens that could affect the crop production, and the effect of biotic factors and abiotic factors on yield production, the effect of detected disease in late stage, and the effect of similarity of symptom for some disease symptoms on grove management. Finally, several methods to connect crop growth with remote sensing observations are discussed.

CHAPTER 1
GENERAL INTRODUCTION

Remote Sensing Technique

Remote sensing is a technique that deals with objects and gets information without physical contact. The quantity of reflectance and emitted incident light could be the most important indicators to give information about the subject that has been detected; after that could be applied the process information in real condition. So when the light strikes the target, a number of things could occur. The light could be converted to energy because the object absorbs part of incident light, the second option the target could reflect the incident light, and the third option the light wavelength could be transmitted by the object. Man eyes can see the visible light which is reflected by the object. For example, we can see green color for plant because the most amount reflection is visible in green range (500-600 nm). Any change in light reflectance could decrease or increase green light reflectance, because objects have a tendency to selectively absorb, reflect, or transmit light at certain frequencies. As I mentioned, this happening in vegetable subject might reflect green light while absorbing all other frequencies of visible light in optimal case. On the other hand, some targets might selectively transport blue light while absorbing all other frequencies of visible light. The way in which visible light relates with an object is reliant on the incidence of the light and the nature of the particles of the material.

Visible Light Absorbed, Reflected, and Transmitted

This section will focus on why the object reflected or emitted some bands, so absorbing, transmitting, and reflecting light will be studied to know what the very important factors could effect on light incident and thus give information about the target situation. Any material contains atoms and molecules, and those contain electrons. Each electron has a tendency to vibrate at particular bands region. When a light bands with that same normal frequency imposed

upon an atom, then the electrons of that atom will be set into vibrational signal. If a light wave of a certain frequency strikes a substance with electrons having the same vibrational incidences, then those electrons will absorb the energy of the light wave and convert it into vibrational wave. In this case, the vibration energy will transfer to thermal energy instead of vibration motion. Therefore, the light incident of that given frequency is absorbed by the target; it is not possible to be released in the form of light. So the discriminatory absorption of light by exact substantial happens because the certain frequency of the light wave equals the frequency at which electrons in the atoms of that material vibrate. As we know, each atom and molecule has specific frequencies of vibration, so the light absorption varies depending on vibration intensity and, thus, will effect light selective absorbance. On the other hand, if the frequencies of the light bands do not match the natural frequency of vibration of the materials, then reflection and transmission will occur. Because of incompatibility between light incident and material electrons, the energy will be reemitted and reflected as light wave. The science scholars noticed the light property and applied the remote sensing technique. The color of object comes from light reflectance or diffusion to our eyes. So, if an object absorbs all of the frequencies of observable light except for the frequency associated with green light, then the object will appear green in the presence of ROYGBIV. And, if an object absorbs all of the frequencies of observable light excluding the incidence related with red light, then the item will look red in the attendance of ROYGBIV.

Disease Detection Technique

Disease in plant causes economic issue worldwide, especially for the agricultural industry. There are some diseases that kill all plants in a few days or weeks. There are many methods to detect disease or insect depending on availability of instruments in the field.

Scouting

Farmers commonly use scouting to detect disease plants but this method is time-consuming and needs more laborers, especially for large area, so it is not precise. In some cases, the disease has the same visible symptoms of other diseases or nutrient deficiency; the human eyes cannot differentiate the cause of the disease. In some cases, dogs are used to help find disease by sniffing out pests or use aerial scouting by using helicopters to fly around the field, but this method is considered as inefficient and expensive (Kuflik et al., 2008, Hammond et al., 2006, Burgess, 1983). Scouting or routine field inspection needs people that have experience and attained some courses to learn how to detect disease; this study, training course increased the productivity of cotton crop. In Mexico and Central America countries, scouting is used to inspect infested cotton crop, but not for a huge area, they used only in limited area; recently, very few farmers used scouting for huge area. In some circumstances, scouting is applied to test pesticide management in small area (Matthews, 1996). (Allen and Roberts, 1974) studied the cost effectiveness and time-consuming per acre in different area and different season; they found the laborers need 4 to 6 weeks to cover 24 and 27 acres, respectively. In addition, the cost of each acre was 5.5¢/acre/week. It is clear that scouting or naked eyes detection needs large number of laborers and high cost and time-consuming than other techniques.

Polymerase Chain Reaction (PCR) and DNA

Polymerase chain reaction (PCR) and DNA is a good investigation method and precise, but are time-consuming and expensive. Each sample needs a long time and complex process to get results. Therefore, early decision is very important to reduce economic damage and control on disease to prevent spreading disease to another area through vector control, pesticide spraying, or eliminates infected plant to protect other plants and, thus, will increase the crop productivity. There are many scholars utilizing PCR method in order for pathogen detection (Henson and

French, 1993, Minsavage et al., 1994, Green et al., 1999, Ahrens and Seemuller, 1992). It was an accurate method (Kinard et al., 1996), but time-consuming and highly expensive (Schneider et al., 2004).

Nondestructive Method

Remote sensing technique use to cover large area in short time to get information in early disease stage to make the right decision. Visible near infrared spectroscopy on this method might be used in the field. In order to build remote sensing, you should first develop ground base sensor system to monitor stress and plant health (Sankaran et al., 2010b). From previous review, monitoring plant can be divided into two methods, destructive and nondestructive. In this project, we focused on the nondestructive method such as spectroscopy and imaging technique.

VIS-NIR spectroscopy

In remote sensing, a sensor is used that can detect the light that might be reflected, transmitted, and emitted when the human eyes would be unable to feel the light in some wavelength, especially in near infrared and microwave wavelength. The electromagnetic spectrum varies from shorter wavelengths to longer, so the light wavelength can be divided into several types: visible (400-700 nm), near infrared (700-1300nm), and mid infrared (1300-3000 nm); this is the most important wavelength. Can be used it in spectrodiometer device to detect disease. However, visible range has short wavelength and high energy, while infrared range has longer wavelength but has less energy.

Spectroscopy indirect and non-distractive method is a very useful method we can use in different ways such as disease detection, fruit quality, nutrient deficiency, soil elements, and different food processing (Zhang et al., 2007, Liu et al., 2003). Menesatti et al. (2010) emphasized that chemical analysis was a destructive method and time-consuming; therefore, he used VIS-NIR spectroscopy to estimate nutrient level N, P, K, Ca, Mg, Fe, Zn, and Mn in orange

leaves in different levels using foliar analysis and pen prop to obtain spectral reflectance for each leaf individually. The result showed high correlation when he used spectroscopy method. Fan et al. (2009) inspected firmness and soluble solids content (SSC) of Red Fuji apples by using VIS-NIR spectroscopy. The experiment was applied in different light source and different fruit orientation; 650-920 nm was applied and two calibration models were applied based on partial least square and obtained 86% classification correctness and r^2 0.95. Camps and Christen (2009) examined the capability of portable VIS-NIR spectroscopy to decide apricot quality; the parameters used in this test were soluble solids content (SSC), total acidity (TA), and firmness (Fi) and use several varieties. For the second part of the experiment using VIS-NIR handled color intensity with correct efficiency; the results were encouraging to use this technique in the field during postharvest. Sirisomboon et al. (2009) studied the reflectance spectroscopy of VIS-NIR domain (600-1100 nm) to consider the outer such as frozen green soybean, and insect-eaten; while for inner of fresh green soybean pods caused by disease such as downy mildew and anthracnose, they analyzed the data using principle component analysis and they found the spectroscopy method can be used in the green soybean grading process. West et al. (2003) assisted in reducing pesticide and chemical application and to reduce the risk of pollution worldwide by using optical sensor to detect the diseases and spray in infected zone if it is un-necessary to spray the whole field and of course this will lead to economic efficiency in addition to keeping the environment clean. Magwaza et al. (2012) studied probability to verify the quality of citrus using nondestructive method in inner and outer quality measurement, including the selection of NIR characteristics for spectra capture, analysis, and summarized his work that it is possible to use this method in measuring the quality of fruit. Wu et al. (2008) had applied VIS-NIR spectroscopy in lab conditions to identify *Botrytis cinerea* on eggplant leaves

in early disease stage; principle component analysis was used to reduce the frequency of wavelength dimension in some bands, and they performed back propagation neural networks and obtained accuracy rate of 85% in calculating fungal contagions. Huang and Apan et al. (2004) utilized portable spectrometric VIS-NIR range (400-1300 nm) to investigate Sclerotinia rot disease in celery plant using partial least square regression model; they used raw data and first and second derivative data and they found the same result when they used full range (400-2500 nm). Fu et al. (2007) detected brown heart in pears and compared transmission and reflectance modes of VIS-NIR by using spectrometric in range of 400-1110 nm with two types of varieties and two detectors "(Si: 670-1110 nm; InGaAs: 800-2630 nm)". They implemented data by using discriminant analysis and they found it is possible to detect the disease in spectroscopy with transmission modes that had higher classification value that reached up to 91%. Zhao et al. (2003) performed un experiment to examine the effect of the nitrogen on corn (*Zea mays* L. cv. 33A14) by using different levels of nitrogen and they measured different parameters of leaf hyperspectral reflectance, concentrations of chlorophyll and leaf area and concentration of N; they found there was a high correlation between N concentration and spectral reflectance. Cozzolino et al. (2011b) reviewed new sensor technique using mid-infrared (MIR), near-infrared (NIR), visible (VIS), and ultraviolet (UV) spectroscopy to monitor and improve grape and wine industry. Cozzolino et al. (2011a) also worked on red grape homogenates to examine concentration of minerals such as (Ca, K, Mg, P, S, Fe, and Mn) and electric conductivity (EC) by using NIR spectroscopy in range (400-2500 nm), they pre-processed the data using multiple scatter correction and then used partial least squares (PLS) regression and cross validation . Mg, S, and EC in grape could be figured out by using NIR reflectance technique. Ulissi et al. (2011) tried to avoid the expensive cost of using different analyzing

methods and compared to spectroscopy method; in this research they measured N concentration in "chemical standard analyses, chlorophyll meter readings, and N-NO_3 concentration in petiole sap" and compared the result with VIS-NIR spectroscopy. The correlation between predicted values from spectral reflectance analysis and the practical chemical standards showed, in the independent assessment, extremely significant correlation coefficient (r = 0.94). Min et al. (2006) conducted the experiment in the field to estimate N level in the leaves of Chines cabbage. They also investigated N and water content in chemical standard method to compare the result with reflectance spectral method. Three different levels of N were used (40%, 80%, and 100%). Correlation coefficient spectrum, standard deviation spectrum, stepwise multiple linear regression (SNMR), and partial least squares (PLS) regression were used to decide wavelengths for N estimate models. They found there were significant correlation between water content and N prediction and they selected some bands that can be used to predict N deficiency (550, 840, 1467, 1910, and 1938 nm). Ceccato et al. (2001) studied leaf level by using spectral vegetation index in short wave infrared. They didn't get good results without use of another parameter (inner structure and dry substance to approach reasonable result). Also, they used near infrared wavelength combination with short wave. The aim of this research was to investigate the potential and approaches for using visual remote detecting. Cheng et al. (2006) utilized three vegetation indexes to find out the relationship between canopy water content and Equivalent Water Thickness (EWT). EWT was investigated using the MODTRAN-based suitable technique which was used to estimate their impact on the water content approximations. Thenkabail et al. (2000) studied the best bands and what was appropriate for describing agricultural yield biophysical variables for different crops (cotton, potato, soybeans, and sunflower) by using reflectance measurement in range 350-1050 nm. Three different reflectance methods were used:

optimum multiple narrow band reflectance (OMNBR), narrow band normalized difference vegetation index (NDVI). The best waves were collected in long and short wavelength (500, 550, 650, 700, 900, and 950 nm). The aim of Thenkabail et al. (2004) research was to utilize spectral reflectance in range 400-2500 nm to estimate the vegetation and agriculture crop to reach the best narrow bands to classify different vegetation species such as shrubs, grasses, weeds, and four species from ecoregions of African savannas. Three classification methods were used. The significant accuracy classification was hyperspectral narrow bands because it was increasing the accuracy 9% and reached up to 43% to classify vegetation crop species.

Hyperspectral and multispectral image

Kuo et al. (2014) insisted use of hyperspectral imaging in general life purpose-not only in agriculture such as astronomy, medicine, food safety, forensics, and target detection. Qin et al. (2009) studied the ability of hyperspectral imaging to recognize canker disease from normal citrus fruit and infected citrus fruit; the spectral range they performed was between 450 and 930 nm. Spectral information divergence classification method was used and they obtained overall classification accuracy of 96%; therefore, they confirmed that it is possible to use hyperspectral image to recognize citrus canker from other diseases that had the same symptoms. Li et al. (2014) proved the capability of hyperspectral imaging as an efficient method to detect Huanglongbing disease in citrus. Extended spectral angle mapping (ESAM), Mahalanobis distance, and an unsupervised method, K-means, were used as classification methods. The first method (ESAM) was the highest classification value at about 86%. Dong et al. (2014) detected thrips defect on green-peel citrus. They had selected 4 bands that could detect the disease in principle component analysis (PCA) in VIS-NIR region (523, 587, 700, and 768 nm); however, they obtained 96.5% classification accuracy for both methods PCA and B-Spline lighting correction. From this result, they confirmed that it is possible to recognize thrips disease in this

method. Kumar et al. (2012) had used both hyperspectral and multispectral images in order to detect citrus greening disease. The experiment was conducted in two time periods, 2007 and 2009, from different groves. PCR method and portable spectrometric were used to validate image result. Two different soft wares were used (ENVI, ITT VIS) for hyperspectral image analysis. HLB infected areas were recognized using image-derived spectral library, "mixture tuned matched filtering (MTMF), spectral angle mapping (SAM), and linear spectral inmixing." MTMF was the highest accuracy, then others. The precision of SAM using multispectral images was 87%. It was the highest value compared to other methods. Okamoto and Lee (2009) tried to detect HLB citrus disease for the varieties Tangelo, Valencia, and Hamlin. The authors found interesting result to identify the disease relatively with varieties. The fruit detection tests revealed that 80-89% of the fruit in the foreground of the validation set were recognized correctly, though many highly discriminated fruits were identified wrongly. Multispectral and fluorescence images were utilized in this study to detect yellow rust in wheat crop; the overall error was less in image fluorescence detection. In general, quadratic data analysis was a higher classification value than Self-Organizing Map; it reached up to 95% (Moshou et al., 2005).

CHAPTER 2
BACKGROUND AND LITERATURE REVIEW

Review on Laurel Wilt Disease, Biotic and Abiotic Factors Have the Same Symptoms

The avocado crop is considered the second largest tropical tree after citrus in Florida, 7000 acres were planted with avocado especially in the south part of the state. Avocado production makes a lot of money every year, reaching many millions of dollars in Florida and California. This high industry benefit is threatened by a new disease called laurel wilt (Lw). This disease has the ability to kill avocado tree through few weeks depending on the severity of the disease. Lw disease has the same symptoms in the early stage that make it difficult to recognize it from other stress, especially with aerial survey. This chapter discusses some factors that affect spectral reflectance, and reviews biotic and abiotic stress and the dynamic of control of these factors.

Factors Affect Spectral Reflectance and Absorb in Leaf Area

There are many factors that could affect spectral reflectance; this depends on leaf structure, water content, mineral tension, age and vigor of canopy, so spectral signature might change according to internal external structure factors, characteristic spectral features verified for the three main visual spectral fields: chlorophyll concentration, cell structure, and water content.

Chlorophyll Concentration

A healthy plant usually has dark green color, because it reflects bands in visible range 450-540 nm because of the chlorophyll content. When the plant absorbs sunlight to process photosynthesis, are absorbed, blue (340-450) nm and red (650-750 nm), while reflecting green color. There are chlorophyll a and b, each one absorbs sunlight in different wavelength, so they both complement each other to provide cells plant with energy that is necessary to introduce glucose and carbohydrates. Gitelson et al. (2003) investigated the relationship between chlorophyll content and spectral reflectance for varices species (maple, chestnut, wild vine, and

beech leaves) and different wavelength range. They found out spectral range between 520-550 nm and 695-705 nm correlated with the chlorophyll concentration for all leaves. Sims and Gamon (2002) tried to improve spectral indices for estimation of leaf pigment content for various species and leaf structure variation to utilize it in nondestructive method for large scale without wide calibration. The result showed there were no significant difference between leaf structure and chlorophyll content in red range. Also, carotenoid and anthocyanin monitors performed poorly for all spectral data. Chappelle et al. (1992) measured the spectral reflectance and concentration of chlorophyll a, chlorophyll b, and carotenoids in soybeans based on absorption light in specific wavebands. The linear relationship was very strong between ratio spectra and concentrations of the photosynthetic colors made the potential to improve a relation analysis of reflectance bands algorithm. Reduced light absorption by chlorophyll apparently amplified the reflectance of the visible wavebands (500-700 nm) (Sinclair et al., 1971) .

Leaf Structure

High reflectance in near infrared region is related to cell structure because of internal leaf scattering and no absorption comparing to visible region. The most definite original variations often happen in the visible spectral region rather than in the infrared because of the sensitivity of leaf pigment to functional disorders (Knipling, 1970). Penuelas and Filella (1998) found that spectral reflectance of healthy plant has different spectral signature in near infrared domain (700-1300 nm) compering to infected plant.. Also, reflectance is directed by structural discontinuities faced in the leaf. Leaf layer is a very important indicator to identify leaf situation in near infrared region. Any change in reflectance slope belongs to leaf structure and ground area (Heermann and Khazenie, 1992, Horler et al., 1983). The position of the red-edge is defined as the position of the main inflexion point of the red-NIR slope. This is often also denoted as the red-edge index. Red edge position between 680 nm to 730 nm is a very critical parameter when utilizing remote

sensing. This region provides more information about the situation of the plant such as chlorophyll content, water and nutrient deficiency, stress condition, and senescence (Baranoski and Rokne, 2005). Sinclair et al. (1971) studied the leaves of six agronomic crops measuring spectral reflectance in fresh and middle stage and in the end of the season. Deviations in the internal structure of leaves might lead to rises in the near infrared wavelength (700-1300 nm).

Water Content

Drought or water stress is a very important indicator should consider when use the remote sensing. Far infrared 1300-2600 nm represents water stress and senescence, and increased reflectance in the far infrared wavelengths (1300-2600 nm) when they had water loss (Sinclair et al., 1971). Tucker (1979) used normalized difference vegetation index with reflectance data between 660 and 860 nm or near infrared region. Gao (1996) had developed another index focused on water loss. Normalized difference water index (NDWI) provided information about plant in range between 860 and 1240 nm. From the result, any lack in water would affect spectral signature in this range. Therefore, it is possible to combine both index (NDVI) and (NDWI) to obtain more information for image (Gao, 1996). Barrett and Curtis (1999) utilized different species and dissimilar leaf morphologies to determine water content in two NIR ranges (700-1300 nm) and middle NIR (1300-2500 nm). Sims and Gamon (2003) confirmed water stress is a very important indicator for remote sensing application. Thin tissue has best correlated with the water content. The significant correlations with water content in three wavelength domains are (950-970, 1150-1260, and 1520-1540 nm).

Symptoms Similarity between Laurel Wilt and Other Plant Disease

Laurel wilt is a vascular infection of redbay (*Persea borbonia* (L.) Spreng.) and other plants in the family Lauraceae in the United States. It is caused by a fungus (*Raffaelea* sp.) that is carried by an unoriginal beetle of Asian origin, the redbay ambrosia beetle *(Xyleborus*

glabratus Eichhoff*)* (Fraedrich et al., 2008). Since the early discovery of the redbay ambrosia beetle nearby Savannah, GA in 2002, laurel wilt has caused high mortality of redbay in Georgia, South Carolina, and Florida (Fraedrich et al., 2008). South Florida commercial avocado was discovered to be infected with laurel wilt in 2011 (Carrillo et al., 2012). The infection starts in the top, plus upper branches dead, wilting, and discoloration foliage in a few weeks. There are external symptoms in the tree stem, when removal of bark from wilted branch sections bare black-to-brown strips of staining in the sapwood and rare ambrosia beetle holes from which the yellowing extended into the neighboring wood. Laurel wilt is a disaster to the marketable avocado production and is a possible threat to the Lauraceae in the world (Mayfield et al., 2008c).

Avocado Scab

Avocado scab is the most significant disease of avocado fruit and vegetation in Florida and is caused by the fungus *Sphaceloma perseae* Jenkins which attacks fresh leaves, tender tissue of the vegetation and fruit, creating spots that produce spores (Pernezny and Raid, 2001). The disease occurs on leaves as separate purplish to dark brown spots (Stevens, 1922).The spots are observable on both sides of the leaf and ultimately the middles my drop out, leaving slight irregular holes fringed with grayish brown tissue. The most dangerous period for fruit contagion is since the period of fruit set until it has reached a third or half of its regular size (Everett et al., 2011)

The disease acts on the leaves as separate spots, angular in form, commonly less than 2 mm in diameter and brown in color. Spots repeatedly occur in groups or might combine to form irregular spots (Zentmyer, 1984).

A   B

C

Figure 2-1. Avocado leaves infected with laurel wilt disease. A) Early stage infected. B) Very late stage and. C) Late stage. Photo courtesy of author, Jaafar Abdulridha.

Figure 2-2. Avocado Scab infected. Photo courtesy of author, Jaafar Abdulridha Cercospora Spot or Blotch

Figure 2-3. Cercospora Spot or Blotch. Photo courtesy of author, Jaafar Abdulridha

Verticillium

The soil-borne disease is naturally related with plants grown on old land upon which are Verticillium susceptible. Leaves are rapidly wilting partially of the canopy, or on the full tree, and the quick death of the plants. The leaves turn brown and remain attached to the branches for an extended period (Zentmyer, 1984, McMillan, 1976).

Algal spot is a disease of little commercial significance to the avocado business of Florida. The prominent greenish-gray spherical spots may be found on a large number of leaves with no obvious permanent harm to the tissue. The elder bad skin become reddish brown due to the masses of maturing forms (McMillan, 1976).

Figure 2-4. Verticillium infected leaves. Photo courtesy of author, Jaafar Abdulridha Algal Spot

Figure 2-5. Algal Spot. Photo courtesy of author, Jaafar Abdulridha

Powdery Mildew

Powdery mildew may develop serious enough in the nursery to permit an application of fungicide. Greenish areas seem on the upper surface of new, increasing leaves which display the distinguishing powdery, and white, spore-bearing growth on the lower surface (Pernezny and Raid, 2001). Infection on mature leaves generally look purplish-brown initially and may or may not be covered with the white, powdery growth. The white surface growth may disappear as the leaf matures and climatic conditions favorable to fungus change (Crane, 2013).

Figure 2-6. Powdery Mildew. Photo courtesy of author, Jaafar Abdulridha Seedling Blight

It occurs irregularly in the summer season. The fungus attacks the tender buds and leaves of nursery-grown trees. The lesions on the leaves are reddish-brown and enlarge rapidly along the larger veins. Lesions on young leaves are brownish-black and frequently cause curling and twisting of the leaves. Terminal buds are killed outright. The symptoms on the young, tender stems are dark, sunken, elongated lesions which occasionally split open (Zentmyer, 1952).

Figure 2-7. Seedling blight. Photo courtesy of author, Jaafar Abdulridha Phytophthora Root Rot

The symptom of this disease: leaves are small, pale green, often wilted with brown tips, and drop readily. Young branch dieback from the tips, and finally the tree is reduced to a bare framework of dying branches. Tree death may take from a few months to several years, depending on soil features, cultural performs, and ecological environments. The minor feeder roots on diseased trees may be absent in the progressive steps of decay. When current, they are regularly dark, brittle, and decayed, in divergence to vigorous trees which have plenty of creamy-white feeder roots (Demelash and Getachew, 2015, Machado et al., 2013).

The symptom of freeze: firm, brittle, dead, and curled leaves, with a brown or bronze, water-soaked/discolored small branches, larger branches and trunks can split and lose bark, discolored fruit, with bronzed to blackened skin, browned buds and flowers, fruit stems can be killed or ring barked, causing heavy-fruit drop (Krezdorn, 1974).

Figure 2-8. Phytophthora Root Rot. Photo courtesy of author, Jaafar Abdulridha

Figure 2-9. Freeze damage. Photo courtesy of author, Jaafar Abdulridha Freeze Damage

Salt Damage

Salinity comes from irrigation with salt water or from increasing the water table or from the soil itself, so it is a serious problem in the world. In southern Florida, sometime avocado trees are flooded with seawater. The first sign that the soil around your avocado tree has too much salt is tip burn on the leaves. The tips of some leaves begin to turn yellow and curl slightly, then the yellow areas travel farther into the leaf and along the sides (Bernstein, 1975). Some leaves might burn in spots on the interior, making brown or yellow circles along the inner vein (Bhatti and Loneragan, 1970). This is sometimes called sodium scorch (Ayers et al., 1952). Although the most visible sign of high soil salinity is leaf tip burn, other things are going on inside your

avocado tree. The salt stunts root growth, keeping the tree from getting the necessary nutrients to produce fruit (Jones, 2012). Excess salt in the soil can change the soil's density, keeping it from draining properly. This can flood the avocado tree's root system and kill it (Linderman et al., 1983). The burned leaves have reduced green surface area, which prevents the tree from performing enough photosynthesis. This reduces the nutrients available to the tree. In addition to reducing the fruit yield, a lack of nutrients can stunt the tree's growth. The burned leaves eventually fall off, forcing the normally evergreen tree to expend energy producing new leaves before it can be healthy enough to produce fruit (Bar et al., 1997)

Nutrient Deficiency

Iron

Iron deficiency is a critical problem for the plant because it effects the growth of tree and the quality of fruits. Iron lack also has an effect on absorbing some important minerals in soil such as phosphorus, copper (Abadia et al., 1999). Leaves turning yellowish is due to reductions in the leaf absorption of photosynthetic colors, chlorophylls, and carotenoids (Abadia et al., 1999). Chlorosis may be caused by a real shortage of iron or by applications of extreme quantities of lime or phosphate to certain soils. It may be caused by flooding, poor drainage, or high levels of certain mineral elements in the soil such as manganese, copper, or zinc. The optical symptoms are often disorganized with other conditions such as a lack of magnesium, manganese, or boron or some other elements. A lack of iron in the soil is unusual but iron can be absent for absorption if soil pH is not between about 5 and 6.5 (Chen and Barak, 1982). Alkalinity of the soil (the pH is above 6.5) is a common issue in the soil that will lead to an effect on iron absorption.

Scholars have studied iron deficiency and the impact of lack and over fertilizer on plants. (Mariotti et al., 1996) studied spectral reflectance when added five rate level from mg L (-1) 0 to

Figure 2-10. Avocado leaves with salinity damage. Photo courtesy of author, Jaafar Abdulridha

4 mg L (-1) of iron to corn and sunflower crops to investigate the effect of iron in remote sensing technique. From the result, it was increased reflectance and diffusion, and shifted the red edge location of reflectance curves in the direction of shorter wavelengths. The symptom of iron deficiency was clearer than sunflower and needs more iron in order to be an optimal planting crop. (Zarco-Tejada et al., 2005) emphasized that it is possible to use remote sensing imagery to detect iron and nitrogen deficiency; canopy reflectance responded to nutrient deficiency.

Figure 2-11. Iron deficiency. Photo courtesy of author, Jaafar Abdulridha

Nitrogen Deficiency

The communed symptoms of nitrogen deficiency: green leaves turn to yellow or pale green and the vegetation part has less density than healthy plant because of being unable to make sufficient chlorophyll. Lower leaves look paler than young leaves, so symptoms would depend on growth age. These symptoms are confusing sometimes depending on soil condition and season, so it is not easy to recognize nitrogen deficiency with other stresses such as deficiencies in other nutrients, toxicity, herbicide damage, disease, insect harm, or environmental situations. Therefore, it is necessary to perform PCR test; as we mentioned, this is an accurate method but is a long process. Spectral reflectance is one nondestructive-alternative method, by measuring chlorophyll level at the field or by using image technique to determine nitrogen deficiency. Nitrogen is a very important element in plant construction; therefore, there are many studies that tried to detect N to determined lower and higher level in vegetation area to complicate the fertilizer application (Noh et al., 2005, Lukina et al., 1999, Goetz et al., 1983). It is possible to monitor different levels of nitrogen in three periods of season for corn crop and weeds, so there were specific bands (from 409 to 947 nm) that were effected in nitrogen stress for weeds and corn depending on growth stage (Goel et al., 2003).

Phosphorus (P) Deficiency

Phosphorus is very important for new plant tissue; any lack of this element will lead to damage of new tissue because it is a component of the complex nucleic acid structure of plants. Plants deficient in P are stunted in development and often have an irregular dark-green pigment. Sugars can store and cause anthocyanin pigments. The most communed symptom is a reddish-purple color. Red coloring may be encouraged by other features such as insect destruction. It is not easy to recognize P deficiency because it has the same symptoms of N and Fe deficiency specially or in early symptom of freeze damage, low temperature could affect soil

to P uptake. Mutangao and Kumar (2007) examined the ability of imaging spectroscopy and neural network map phosphorus concentration. The most common sensitive bands of phosphorous deficiency were in short wave 2015 and 2199 nm. Wiwart et al. (2009) studied three different legume crops under four elements of stress deficiency of nitrogen, phosphorus, potassium, and magnitude by digital color image analysis. All crops had strong response when the color of leaves changed, especially yellow lupine responded to the extreme degree of phosphorus shortage. Early detection could reduce the effect of disease and increase the productivity. When you have a quick diagnosis, then you have act quickly to reduce the risk of late stage for any stress (Chaerle et al., 2007).

Figure 2-12. Avocado leaves with nitrogen deficiency. Photo courtesy of author, Jaafar Abdulridha

Figure 2-13. The symptoms of phosphorus (P) deficiency. Photo courtesy of author, Jaafar Abdulridha

Potassium Deficiency

Yellowing begins at the margin of the leaf and spears toward the veins. Brown spots develop within affected area. The margin associated with some interveinal yellowing on the rest of leaf (Barnard et al., 1991, Haas, 1939). The contrast with salt damage where there is generally little or no yellowing associated with the marginal burn, but potassium deficiency symptom has the same nutrient deficiency symptoms. Lukina et al. (1999) utilize spectral reflectance to determine whether deficiency of Nitrogen (N), Phosphorus (P), Potassium (K), Calcium (Ca), and Magnesium (M) changes spectral reflectance possessions of wheat leaves. Reflectance curve shifted down in visible range and red edge (412-770 nm) when there was lacking in potassium, calcium, and phosphorus. Fridgen and Varco (2004) investigated nitrogen and potassium deficiency in cotton crop by spectral reflectance in various levels in both elements. Partial least squares regression was used to predict the nutrient stress. When the K was sufficient, red edge was shifting toward longer wavelength with increased N supply.

Figure 2-14. Avocado leaves show potassium deficiency. Photo courtesy of author, Jaafar Abdulridha

Magnesium

Magnesium deficiency effect on chlorophyll concentration; therefore, when we have heavy deficiency symptoms, the leaves turn to yellowish color. In fact, Mg is a mobile element, moves from old leaf to new flush to make up shortfall. Therefore, the symptoms appear on old leaves and so on (Cakmak et al., 1994). Basically, these symptoms are the same as some diseases and nutrient deficiency, start with yellowing leaf, so it is necessary to take advantage of electromagnetic spectral technique. Mariotti et al. (1996) confirmed previous study that insisted on spectral reflectance rapid method for disease and nutrient detection. However, in this study, they examined the effect of several element deficiencies such as Fe, S, Mg, and Mn deficiency on reflectance, absorbance, and transmittance spectra of wheat, barley, and corn. All treatments showed reduction of chlorophyll and thus spectral reflectance gave low reflectance and transmission, decreased leaf absorbance, and shift down the red-edge position, defined as the variation point that happens in the quick transition among red and near-infrared.

Manganese

The first appearance is on new leaves because Mn is non-mobile from old leaf to new tissue. Interveinal chlorosis is the most popular symptom. In addition, there are a series of brownish-black spots appearing in the canopy that has a lack of Mn. Young leaves. In minor grains, grayish zones seem near the base of fresher leaves. The symptoms looks like symptoms of another disease or nutrient deficiency, so there are many studies which tried to recognize Mn deficiency and other stresses such as (Bravo et al., 2003, Moshou et al., 2003)

Copper

Leaves with a lack of copper shows pale color, in advance stage leaves dried, curly, weak connection with branches causes die-back, yellow tip, exanthema copper disease of new leaves. Deficiency of copper affects flavor, storage capability, and sugar content of fruits and can affect

productivity as well. It is a really serious problem when we have Cu shortage. Bernal et al. (2007) compared the effect of extra Cu on soybean crop planted in soil and hydroponic method to monitor the change on leaves and root plant. Fluorescence radiation was utilized. The results significantly designate that changed Cu-uptake and transference pathways need function in leaf cells matched with root cells. Liu et al. (2012) applied successfully fluorescent sensing platform for label-free sensitive and selective detection of Cu.

Boron

Carrero et al. (2005) utilized spectrophotometric to detect boron. Azometihine-H-boron complex technique was settled in order to flow boron in soil, fruits tissue, and leaf tissue of coffee plantations from different areas.

CHAPTER 3
DETECTION AND DIFFERENTIATION BETWEEN LAUREL WILT DISEASE, PHYTOPHTHORA DISEASE, AND SALINITY DAMAGE USING A HYPERSPECTRAL SPECTRODIOMETER TECHNIQUE

Introduction

Avocado is the second most important tropical fruit crop in Florida after citrus (NASS/USDA, 2009). The avocado crop is valuable to the state economy, and the avocado industry brings in a substantial amount of "new dollars" to the state, resulting in an overall economic impact of close to $100 million per annum (Evans, 2015). However, the revenue from avocado in Florida has been greatly reduced, 50%, by the effects of laurel wilt (Lw) disease (Evans, 2015, Evans et al., 2014). Lw disease has caused serious losses in fruit quality and quantity, resulting in reduced sales, and an increase in agro-industrial waste, pesticide costs, and management expenses (Evans et al., 2014). Laurel wilt disease has been reported as a major threat to the commercial production of avocado in Florida (Carrillo et al., 2013, Ploetz et al., 2013). One vector of Lw disease is the redbay ambrosia beetle (Evans et al., 2014, Kuhns et al., 2014, Kendra et al., 2014). The redbay ambrosia beetle, *Xyleborus glabratus Eichhoff (Coleoptera: Curculionidae: Scolytinae)* is associated with fungal symbionts such as *Raffaelea lauricola* (Fraedrich et al., 2008, Hanula et al., 2008), a fungi that kills the tree by blocking water flow to the canopy (Kendra et al., 2013).

The secretion of redbay ambrosia beetle saliva helps to spread the fungus *R. lauricola* from tree to tree (Carrillo et al., 2012). In addition, the fungus *R. lauricola* grows rapidly inside the wooden stems (Jeyaprakash et al., 2014, Carrillo et al., 2013). The fungi reduce the tree's ability to transfer nutrients and water to the branches and leaves. Generally, the disease causes the color of the leaves to change from green to a red-purple brown color, the underside of the bark to become black, and small pores and holes to form inside the outermost layer of bark (Ploetz et al.,

2010). All of these symptoms may indicate the presence of the redbay ambrosia beetle in the tree (Ploetz et al., 2010, Fraedrich et al., 2008). Many of the disease symptoms are similar to those caused by other diseases such as Phytophthora root rot (*Phytophthora cinnamomi*) or factors such as lightening damage, freeze damage, or drought stress (Sankaran et al., 2012), making visual detection of Lw difficult. Moreover, the development of external symptoms signifies colonization of the host (Ploetz et al., 2012b). It may not be possible to manage the disease once plants display external symptoms (Inch and Ploetz, 2012). An advanced and rapid method for detecting Lw that can distinguish these biotic and abiotic stresses is therefore needed (Sankaran et al., 2010a). Currently, the only method to manage Lw disease is complete removal of the infected tree, including the root, so that vectors cannot transfer the disease to healthy trees (Evans et al., 2010, Hanula et al., 2008, Sankaran et al., 2012). Lw disease has spread very quickly in just a few years through Florida and other states (Ploetz et al., 2012b), so it is necessary to find a rapid method to detect the disease in a timely manner to at least reduce the spread of the redbay ambrosia beetle. There are several methods to detect the disease such as scouting and polymerase chain reaction (PCR) (Henson and French, 1993). Those methods are costly and time-consuming; therefore, it is necessary to use other methods to detect the disease (Bravo et al., 2003). Spectral reflectance is a method that is rapid and non-destructive (Graeff and Claupein, 2003). Spectral reflectance methods depend on reflected or emitted radiation from different bodies, so each material has a different spectral signature (Curran, 2000). For plant signatures, the spectral reflectance is either increasing or decreasing depending on physical (external) factors such as chlorophyll and pigment concentration which are used as an indicator of the plant condition in the visible range (450-760) nm (Blackburn, 1998, Broge and Leblanc, 2001). There are also interior factors such as physiological structure, condition of the cell wall,

water content, surface roughness, and stoma activity which will effect light penetration through the leaf structure, so spectral signature in the near infrared (NIR) range of 760 to 2500 nm is used to indicate these leaf features (Moran et al., 1997, Pinter et al., 2003).

It is possible to use Visible-Near Infrared (V-NIR) techniques to distinguish healthy from unhealthy leaves (Vrindts et al., 2002, Mahlein et al., 2010). Ma et al. (2012) used a visible remote sensor with different multispectral wavelengths to detect citrus greening. Some studies confirmed that spectrometric methods are more effective, more accurate, less time-consuming, and nondestructive compared to DNA analysis methods (Menesatti et al., 2010, Tomkiewicz and Piskier, 2012). Franke and Menz (2007) utilized spectral data at different wavelengths to monitor the powdery mildew disease of leaf rust at different stages of development. Fungicide treatment was then applied using precision agriculture to determine the interaction of the crop with the fungicide. Results were compared with chemical analysis and showed an increase in early disease detection from 56% to 88.6%, which was considered an acceptable result regarding early disease detection.

The goals of the present study were to i) determine the hyperspectral mean reflectance curves of Lw infested trees at different stages of development and ii) select the optimal spectral bands for discrimination of damage due to Lw, H, Prr, and salinity.

Materials and Methods

Host Plants and Inoculation in Greenhouse

Experiments were conducted in Miami-Dade County in an indoor controlled environment at the University of Florida's Tropical Research and Education Center (TREC) in Homestead, FL. Avocado leaves were obtained from the "Simmonds" variety of avocado trees grown in pots in greenhouse trials where different treatments were used to induce the same symptoms and produce some factors.

Healthy leaves Lw early stage Lw late stage

Prr early stage Prr late stage Salinity early stage Salinity late stage

Figure 3-1. Avocado leaves in different stress stages. Photos courtesy of author, Jaafar Abdulridha

Avocado trees were 1 year old and almost 1 m tall. The pre experiment methodology for each treatment is explained below:

Laurel wilt (Lw): Ten plants were inoculated with Lw at approximately 5 cm above soil level by drilling four small holes around the circumference of the trunk, each hole receiving 25 µL of a *R. lauricola* spore dilution at a concentration of 30, 000 colony forming unit (cfu)/mL for a total of 3, 000 cfu/plant. Holes were sealed with paraffin wrap. For the early inoculated stage of Lw, new shoots were wilted and the leaf color changed from a dark oily green to light green on most, while others turned fully yellow.

Salinity (Sln): One liter of salt solution was applied to each tree. The sea water was similar to that of the sea water from the east coast of Florida with a salt concentration of 36 g/L. Leaves showed some browning symptoms after a few days. Then, another liter of the sea water

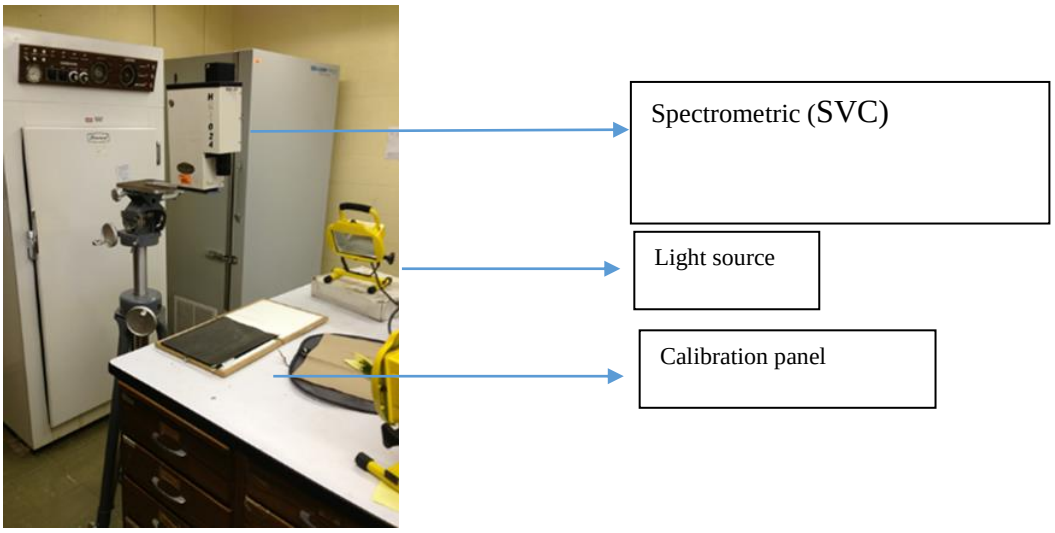

Figure 3-2. Laboratory setup including spectrodiometer and halogen light sources. Photo courtesy of author, Jaafar Abdulridha

was applied on experimental day 17. Further, browning symptoms were fully developed, similar to those of leaves affected by Lw.

Phytophthora root rot (Prr): Ten plants were inoculated by infecting 10 pots with 6 grams of wheat seed colonized with *Phytophthora cinnamomi*. After 14 days, a very few early symptoms of Prr appeared in the form of the yellowing of some leaves.

Control (H): These plants were grown in full sun.

During the early growth stage, the plants showed few symptoms or a symptom of Lw and Prr, so some leaves did not turn to totally yellow, especially those infected with *Phytophthora cinnamomi*. However, during the late stage, the plants showed many symptoms of Lw and Sln such as discoloration and necrotic leaves depend on the severity of the stress factor. Figure 3-1 shows bunch of the tested avocado leaves during these two stages.

Spectral Data Collection

Forty leaves were sampled from each of the control (H) and treated plants. Multi scans were taken at different positions in order to reduce the variability of the device and the leaves.

Five reflectance spectra per each leaf were collected at different stages of symptom development: early stage, and late stage, depending on symptomatic appearance. A handheld spectrodiometer (SVC HR-1024) (Spectra Vista Cooperation, NY, USA) with a 4° field-of-view optical lens in the spectral range of 350 to 2500 nm was used. Two portable halogen work lamps (500 W) were used as the light source, and the reference reflectance spectra were acquired using a white reflectance reference panel (Spectralon Reflectance Target, CSTM-STR-99-100; 168 Spectra Vista Corporation) (Figure 3-2). A spectral data was used in visible and near infrared domain from 350 to 950 nm. Spectral data were averaged to 10 nm and 40 nm, and used based on (Thenkabail et al., 2000, Thomasson et al., 2001), as well as the available waveband filters on the market that would be cost-effective during sensor development.

Data Analysis and Classification

SPSS software (SPSS 13.0, Inc., Chicago) was utilized in this study for spectral analysis. Discriminant analysis and two neural networks, i.e., multiyear perceptron (MLP) and radial basis function (RBF), were used to classify H, Lw, Prr, and Sln based on the 10 nm and 40 nm averaged reflectance data. The classifications were conducted in two stages of disease development: early and late. The analyses were performed independently for the early and late stage spectral data, as well as in a data set composed of all of the reflectance data in order to select the best bands for different development stage.

Stepwise discriminant analysis (STEPDISC)

Discriminant analysis permits the setting up of a predictive model of group membership based on characteristics observed in each case (Franke and Menz, 2007). This method determines significant differences between variables so that repetitive variables can be eliminated (de Castro et al., 2012). The STEPDISC procedure combined forward selection and backward elimination of the variables; forward selection was employed for the inclusion of a

variable, and backward elimination was used for the removal of variables no longer significant in the model (de Castro et al., 2012). A Wilks's lambda was performed to determine the significance of each discriminant function; the lower the Wilks's lambda value, the greater the spectral differentiation between groups (Karimi et al., 2005). Thus, at each step, the variable that minimized the overall Wilks's lambda was entered (Franke and Menz, 2007). The data were randomized and separated into two independent parts: one was used to develop and construct the model; the second was used to validate the accuracy. The data set was divided into 30% for training and 70% for validation.

Neural networks

Artificial neural networks operate by machine learning, in that inputs and outputs are given to the network one at a time, and the network incrementally improves a model to approximate the input/output function (Thenkabail et al., 2005). Once the neural network has learned to carry out the desired function, the input values can be entered and the neural network will calculate the output (Franke and Menz, 2007). Two neural networks were used: multilayer perceptron (MLP) and the radial basis function (RBF).

The MLP neural model is a fully connected multilayer feed-forward supervised learning network trained by a back-propagation algorithm which reduces the quadratic error standard (Franke and Menz, 2007). In the MLP, no values are fed back to earlier layers, and the dimensions of the MLP is described as size of input layer × size of hidden layer × size of output layer (Park and Sandberg, 1993, Keranen et al., 2003). In this study, the input layer was the spectrometric data of H, Lw, Prr, and Sln leaves.

The RBF is also a fully connected feed-forward neural network with an input layer, a hidden layer, and an output layer (Franke and Menz, 2007). The variables of the input and output layers were the same as those used in the MLP method. The main differences between these two

neural networks are that in the RBF, the associates between the input and output layers are not weighted, and the transfer purposes on the hidden layer nodes are radially symmetric (Jayawardena et al., 1997). The capability of MLP and RBF for every classification model was determined by a hold-out cross-validation method. Cross validation consecutively classified all variables, but the first one to develop a classification function and then classify the variable was left out (Burks et al., 2005). The full dataset was randomly split into three datasets by partitioning the active dataset into training, testing, and holdout samples.

Results

Figures 3-3 A, B, and C, respectively, show the spectral signature of the early and late stage disease development of Lw, Prr, and Sln as well as H. There were apparent reflectance differences in the red-edge and NIR regions for early and late stage development for all treatments. Higher differences were found between the late stage of each treatment and the healthy plants, suggesting the potential to discriminate disease at that level of decline. Spectral signatures at the early stage are very similar to those for H and were therefore more difficult to discrimination at that stage of development by observation. In the late stage, external symptoms had developed, leaves were wilted or desiccated and were a dull gray-green or brown color while leaves in the early stage were still green, just beginning to lose turgidity.

Early Stage

Figure 3-3 C for the early stage of the Sln treatment shows higher reflectance values in the near infrared domain than for late stage, typical of green vegetation. The same trend occurred for other diseases (Figure 3-3 A and B). Figure 3-3 C shows a similar spectral signature for H and Prr at early stage, since after 14 days, very few early symptoms of Prr appeared. Figure 3-4 shows the comparison between H spectral, Lw signature and each of the other diseases, Prr, and Sln at both stages. Figure 3-4 A shows the reflectance of different bands for H, Lw, and Prr and

did not show a significant difference for spectral reflectance in the blue bands. On the other hand, Lw disease always exhibited lower reflectance in the NIR domain (750-950) than H and other diseases.

Table 3-1 shows the classification results obtained from MLP and RBF for 10 nm and 40 nm bandwidth data. The results obtained with MLP were better than those achieved with RBF, with correct classification percentages ranging from 96% to 99% in all stages and comparisons (Table 3-1). RBF obtained the lowest classification rate (65%) for 10 nm at early stage between H, Lw, and Sal. Table 3-2 shows the classification result for STEPDISC analysis and the bands that were chosen on the basis of their order of entry into the STEPDISC procedure selection to discriminate between healthy, Lw, Sln, and Prr leaves at early and late stages. The most frequently selected wavelengths were found in the red-edge range (717-750 nm) for the 10 nm bandwidth, and in the red-edge and blue for 40 nm. In each of the cases studied, a small Wilks's lambda (0.2-0.0) was obtained, indicating the high discriminatory power of every set of selected wavebands.

Late Stage

The development stages of Lw disease varied in the visible and NIR ranges. The late stages had high reflectance in the 1300-2500 nm range. The late developmental stage showed a lower reflectance in the NIR range of 700-950 nm. Reflectance curves for plants affected by Sln varied from stage to stage depending on salinity concentration. Figure 3-3 C which shows Lw's spectral reflectance in the visible range from 550 to 700 nm increased during the late stage. Lw's late stage showed a significant difference in spectral reflectance spectra for healthy plants. The Prr late stage displayed lower reflectance than that of the healthy plants (Figure 3-3 B). The spectral signature curve showed variation in reflectance values, especially for Prr late stages in the NIR

domain. Percentage was 98-92% for all MLP. STEPDISC was the second-best method, with RBF being the worst of the three classification methods.

Combination of Early and Late Stages

Table 3-4 shows the MLP and RBF classification results for the early and late development stages together for the 10- and 40-nm bandwidths. RBF produced a low value and a high value of classification for the combination of H, Lw, and Prr 40 nm (65%) and (71%), respectively. MLP resulted in a high classification value for the combination of H, Lw, and Prr at 10 nm, while the combinations of H, Lw, and Sal at 40 nm and H, Lw, and Prr at 40 nm had the lowest value. NIR

Table 3-1. Hyperspectral classification of laurel wilt (Lw), healthy (H), Phytophthora root rot (Prr), and salinity damage (Sal) and best band selection using MLP and RBF classification for different stages.

Stage and Parameter setting	Importance variable (nm)	Neuron of hidden layer	Neuron of output layer	Over all classification (%)
Early stage 10nm				
MLP - H, Lw, Sal	717, 750, 739, 526, 952, 772	1	10	96
MLP - H, Lw, Prr	750, 739, 952, 728, 717, 772	1	10	96
RBF - H, Lw, Sal	615, 627, 649, 660, 671, 681	1	8	65
RBF - H, Lw, Prr	794, 806, 783, 817, 705, 693	1	10	71
Early stage 40 nm				
MLP - H, Lw, Sal	738, 780, 944, 615, 697, 656	1	7	97
MLP - H, Lw, Prr	491, 780, 697, 944, 615, 862	1	7	97
RBF - H, Lw, Sal	944, 697, 903, 615, 738, 862	1	10	73
RBF - H, Lw, Prr	409, 421, 433, 445, 457, 469	1	6	60
Late stage 10 nm				
MLP - H, Lw, Sal	885, 874, 952, 852, 841, 761	1	6	99
MLP - H, Lw, Prr	491, 780, 697, 944, 615, 862	1	6	99
RBF - H, Lw, Sal	761, 874, 885, 728, 952, 739	1	10	77
RBF - H, Lw, Prr	409, 421, 433, 445, 457, 469	1	10	97
Late stage 40 nm				
MLP - H, Lw, Sal	862, 780, 738, 944, 410, 903	1	9	98
MLP - H, Lw, Prr	862, 738, 410, 944, 697, 903	1	9	97
RBF - H, Lw, Sal	738, 944, 903, 410, 862, 697	1	7	77
RBF - H, Lw, Prr	410, 532, 450, 574, 38, 862, 697	1	8	93

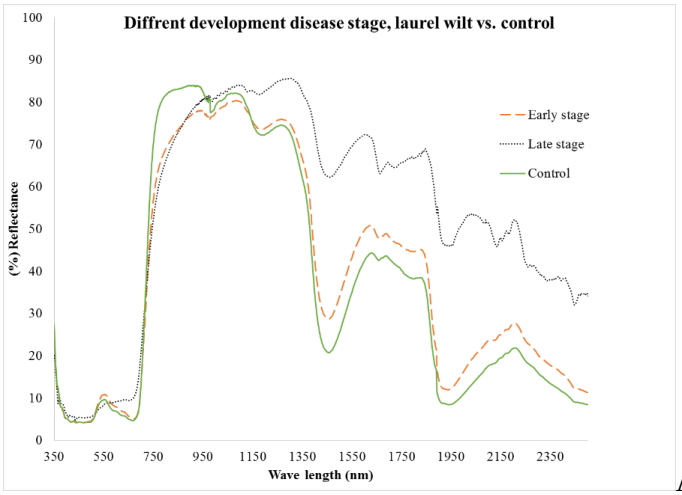

A

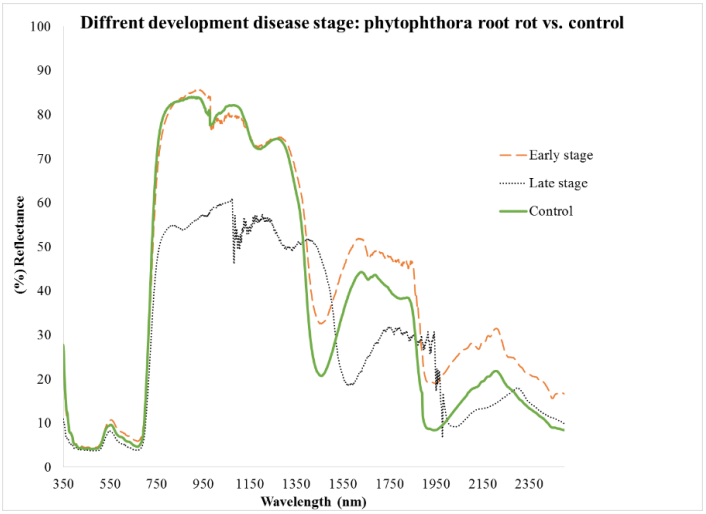

B

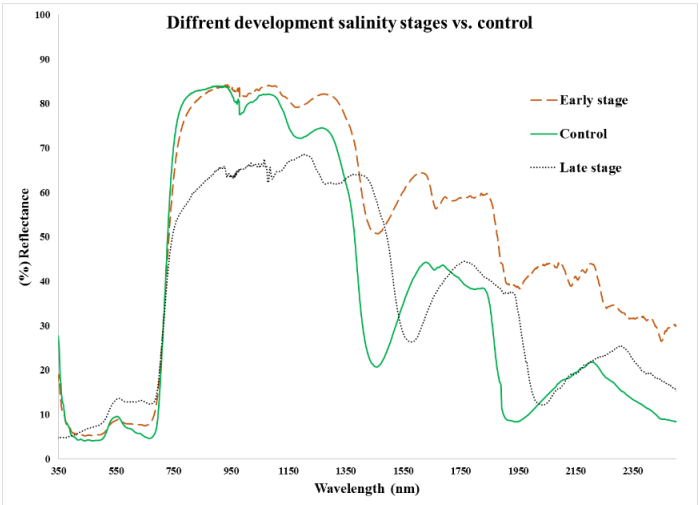

C

Figure 3-3. Spectral signature for A) laurel wilt, B) phytophthora root rot, and C) salinity damage in early and advance stages.

(700-900 nm) was the most frequent range, especially the red-edge, with the exception of the combination of H, Lw, and Prr at 10 nm under MLP for which the blue and green bands were the most common (445, 515, 504, 433). Stepwise classification values are shown in Table 4. The lowest classification in Table 4 is that of the combination of H, Lw, and Sal at 40 nm having a cross validation value of 80%. The average of all categories at 10 nm had a higher value than the average of the categories at 40 nm. The wavebands between 700 and 800 nm were the most common for all categories. The correct classification percentage was 98-92% for all MLP. STEPDISC was the second best method, with RBF being the worst of the three classification methods.

Table 3-2. Hyperspectral classification of laurel wilt (Lw), Healthy (H), Phytophthora root rot (Prr), and salinity damage (Sal) and best band selection using STEPDISC analysis for different stages

Stage	Input data	Best bands selected	Wilks's Lambda	Cross validation (%)
Early stage 10 m	H, Lw, Prr	806, 761, 548, 638, 885, 941, 537	0.2	82
	H, Lw, Sal	908, 745, 852, 504, 445, 638, 604	0.2	86
Early stage 40 nm	H, Lw, Prr	618, 781, 822, 904, 657, 575, 410, 740, 451, 945, 493	0.2	83
	H, Lw, Sal	595, 904, 781, 410, 534, 740, 698, 657, 616, 493	0.2	82
Late stage 10 nm	H, Lw, Prr	817, 829, 761, 409, 941, 548, 560, 421	0.0	98
	H, Lw, Sal	560, 761, 806, 750, 885, 829, 409, 421, 504593, 515	0.05	92
Late stage 40 nm	H, Lw, Prr	817, 829, 761, 409, 941, 548, 560, 421	0.0	98
	H, Lw, Sal	560, 761, 806, 750, 885829, 409, 421, 504, 593, 515	0.05	92

Table 3-3. Reflectance classification using MLP and RBF methods for H, Lw, salinity, and Prr in early and late stage combined.

Stage and parameter	Importance variable	Neuron of hidden layer (nm)	Neuron of output layer (nm)	Overall Classification (%)
H, Lw, Sal - 10 nm - MLP	750, 717, 433, 705, 772, 693, 604	1	9	94
H, Lw, Sal - 10 nm - RBF	705, 537, 548, 409, 717, 560, 526, 941, 952, 433, 615	1	9	67
H, Lw, Prr - 10 nm - MLP	445, 515, 504, 433, 638, 705, 750, 817, 421, 739, 952, 493, 615, 761, 604	1	8	98
H, Lw, Prr - 10 nm - RBF	671, 681, 660, 649, 638, 693, 627	1	8	71
H, Lw, Sal - 40 nm - MLP	738, 780, 944, 862, 903, 450	1	7	93
H, Lw, Sal - 40 nm - RBF	944, 903, 862, 738, 656, 532, 450, 820, 491, 615, 574, 410, 780, 697	1	9	70
H, Lw, Prr - 40 nm - MLP	944, 821, 656, 862	1	8	93
H, Lw, Prr - 40 nm - RBF	944, 697, 903, 532, 738, 656, 574, 615, 862, 780, 821, 410	1	8	65

Table 3-4. Classification reflectance result using STEPDISC for H, Lw, salinity, and Prr in early and late stage combined.

Input data	Best bands selected (nm)	Cross validation (%)
H, Lw, Sal - 10 nm	772, 794, 504, 548, 705, 638, 693, 681, 604, 717, 615, 445	87
H, Lw, Prr - 10 nm	750, 885, 829, 952, 548, 649, 693, 638, 705, 537, 515, 681	89
H, Lw, Sal - 40 nm	780, 820, 491, 532, 944, 410, 574, 697, 450, 656	80
H, Lw, Prr - 40 nm	780, 862, 944, 532, 574, 738, 697, 656, 410, 450, 615	81

Discussion

The chlorophyll and pigment in leaves strongly absorb blue and red light in order to conduct the photosynthesis that is necessary for plant metabolism, meaning that any change in concentration of the chlorophyll will lead to changes in spectral reflectance depending on the pigment ratio (Chernick et al., 1988, Carter and Knapp, 2001). NIR domain reflectance can provide good indicators of cell structure damage to leaves caused by disease, drought, and nutrient deficiency. Any overall change in the leaf will impact the spectral reflectance which would be good indicators to use in hyperspectral detection methods (Broge and Leblanc, 2001, West et al., 2003). The spectral signature for healthy plants had high absorption in red, green, and blue, with a green peak at 550 nm. Each stage had unique spectral reflectance signatures, indicating a relationship between spectral signature and the appearance of disease symptoms.

The main purpose of this study was to select bands that can be used to differentiate between healthy, laurel wilt diseased, salinity damaged, and Phytophthora root rot infested trees. Several wavebands were obtained for each category depending on the severity of the disease or salinity level. There are many studies on band selection to obtain best bands in the VIS-NIR to reduce the huge number of narrow bands, minimize redundancy, and to obtain a statistic model without a long process, i.e., a smaller data set would be more convenient and more efficient in hyperspectral analysis (Gamon and Surfus, 1999, Chang and Liu, 2014). The MLP classification method resulted in classification values for all these treatments. This is related to the progressive nature of disease development, which makes it easier to differentiate the late stage than the early stage. Earlier detection can prevent extensive damage to plants. By detecting disease at the early stage, particularly before symptom onset, growers can spray or remove the affected tree before the disease spreads to the rest of the grove. It is very difficult to recognize laurel wilt symptoms because there are other factors which cause the same symptoms during the early stage. The

results from this study can be used to develop image processing analysis methods for real-time specific disease management. The use of inexpensive remote sensing techniques and aerial images can then be used over large areas to help reduce the damage caused by laurel wilt diseases. The result of this study agrees with the results of other studies using classification methods (Franke and Menz, 2007). Classification values were higher in the late stage than in the early stage for the purpose of combining the early stage and late stage data to obtain wavebands could be used in early and late stage at the same time because not all tree leaves show a lot of symptoms at the same time. The observation of symptom depending on severity of disease and disease development stage (Blackburn, 1998, Pant et al., 2014). Environmental factors and the population of the vectors also affect the dynamic disease transmission in plants (Ploetz et al., 2010, Sankaran and Ehsani, 2012, Garrett et al., 2006). Lw disease showed symptom in different position start on the top of tree and then separate to other part of canopy. Fast decision-making and time-effective spraying at specific locations will lead to preservation of the environment. Accurate band selection and classification are important to encourage the grower to use these methods for timely and appropriate decision making. This is the first instance in which the spectral signature of leaves from avocado trees has been used to determine spectral reflectance and to recommend appropriate bands to detect laurel wilt disease and other factors.

Conclusions

Results from this study showed that it is possible to classify laurel wilt, Phytophthora root rot, and salinity damage from healthy trees using hyperspectral signature analysis at 400-950 nm under laboratory conditions for early stage and late stage in 10 nm and 40 nm interval bands. The most common bands selected for the early stage were 638, 781, 410, 451, and 493 nm. The most common bands for the late stage were 817, 829, 761, 409, 941, 548, 560, 421, 806, and 750 nm. When the stages were combined, the best bands selected by MLP methods were 750, 705, 445,

671, 738, and 944 nm. MLP was found to be the best classification method, with classification value reaching up to 98% in some stages using both 10 nm and 40 nm bandwidths. It is possible to use this method to classify avocado stress conditions in future studies using hyperspectral imaging or other remote sensing techniques. Ten-nm and 40-nm filter bands are inexpensive filters that can be used in remote sensing to reduce the cost of monitoring system. The selected bands can be used in a camera with 6 or 4 bands and can be used for future image processing to reduce the cost and time associated with scouting. These results could be very useful in sanitizing groves by eliminating infested trees completely from the orchard, as currently there are no inexpensive fungicides or pesticides that control laurel wilt.

CHAPTER 4
DETECTION OF LAUREL WILT DISEASE AND NUTRIENT DEFICIENCY FOR AVOCADO TREES USING SPECTROMETRIC TECHNIQUES

Introduction

Laurel wilt (Lw) is a vascular disease caused by *Raffaelea lauricola*, a fungal symbiont vectored by the redbay ambrosia beetle *Xyleborus glabratus* (Carrillo et al., 2013, Moshou et al., 2005). *R. lauricola* affects members of the Lauraceae plant family by inhibiting the flow of water and nutrients (Ayala-Silva et al., 2012, Bates et al., 2013). Lw has killed many thousands of avocado trees, which has caused significant economic losses (Hanula et al., 2008). Profits for the avocado industry dropped from $356 million to $183 million, about 50% of total avocado production (Evans et al., 2010). Lw was first reported in the United States in 2002, and rapidly spread to other states. It was first observed in commercial avocado production in Miami-Dade County in 2011 (Ploetz et al., 2012b). The symptoms of Lw disease are not distinct from other diseases and nutrient deficiencies. The leaves turn from oily green to red or purple color in early stages and progresses to gray and brown in later stages of the disease. An entire tree can die in less than 60 days, after which the leaves can remain on the branches for over a year. Early detection of infected trees is critical because the disease can kill the entire tree within a few weeks. Sanitation is the best method for mitigating disease spread, which requires removing the tree and chipping it, as well as destruction of the roots to prevent root graft transmission (Ploetz et al., 2012b). It is not easy to recognize the symptom of Lw from nutrient deficiency symptom, especially in the early stage, so monitoring for the early detection of nutrition deficiencies in avocado trees would help identify the amount of fertilization needed to prevent damage from malnutrition. Monitoring nitrogen, iron, magnesium, and phosphorous can also prevent excessive fertilization, which is costly and causes environmental pollution (Gunkel et al., 2007, Boroujerdnia et al., 2007). Traditional plant tissue analysis is a very accurate method for crop

nitrogen stress detection, but these methods are time-consuming, labor-intensive, and costly (Huang and Schulte, 1985). Therefore, new techniques for identifying the nutritional requirements of plants are needed for cost- and time-effective management of large areas (Vina et al., 2004). Remote sensing is capable of covering a large area in a short time (Reyniers and Vrindts, 2006). Osborne et al.(2004) used multispectral to detect nitrogen deficiency to assist growers in making management decisions for maintaining proper nitrogen levels within their plants. Feng et al.(2006) emphasized the importance of using multi-band (red, green, blue, and near-infrared) to monitor nitrogen levels, especially when applying precision crop production management operations to obtain accurate information. Noh and Zhang (2012) recommended using multispectral bands to manage nitrogen application, and use of precision agriculture to add the proper amount of fertilizer to specific locations. Thus, the system can minimize the amount of nitrogen leached into the soil, and potentially increase production yield. Moshou (2005) detected yellow rust disease using a hyperspectral sensor between 450 and 900 nm and fluorescence imaging, and was able to identify the disease in its early stages before visible symptoms appeared. Two classification methods were used, quadratic discriminant analysis (QDA) and self-organized mapping (SOM), with the latter method having fewer error classifications that reached 1%. Bauriegel et al. (2011) studied the possibility of detecting wheat infected with *Fusarium* ssp. in the early stages of disease before separating to whole field by using 400-1000 nm spectral sensors indoors. Principle component analysis and 'Spectral Angle Mapper' (SAM) were used to classify the disease in different growth stages to determine in which stages discrimination of *Fusarium* ssp is possible. Apan et al. (2004) determined the relationship between water content in the leaves and orange rust disease in sugar canes using VIS-INR spectroscopy. They found a high correlation between water stress and infection of the

leaves with orange rust disease using “Disease - Water Stress Indices”. Osborne et al. (2002a) determined it is possible to detect nutrition deficiencies such as N and P in corn (*Zea mays.* L.) using VIS-NIR spectroscopy, especially in green and red bands in different growth stages with four different N rates (0, 67, 134, and 269 kg N ha (-1)) and four different P rates (0, 22, 45, and 67 kg P ha (-1)). Zhoa et al. (2005) determined N deficiency on Sorghum using photosynthetic rate (Pn), chlorophyll (Chl), and N concentrations, and hyperspectral reflectance to differentiate N levels at different stages and compared the results. They found a significant relationship between Chl and N concentrations with red and green wavelengths at the red edge in the reflectance spectral curve. Osborne et al. (2002b) utilized spectral radiance techniques to determine water stress and N at various stages with five N rates (0, 45, 90, 134, and 269 kg N ha (-1)), and found there were three wavelengths, 510, 705, and 1135, that could distinguish N deficiency without water stress. Tarpley et al. (2000) applied reflectance indices to diagnose N levels in cotton leaves at multiple growth stages. They discovered that NIR and red edge bands (700, 755, 920, and 1000 nm) had better results and higher accuracy than the chlorophyll content method. Strachan et al. (2002) tried to differentiate the morphological status of corn crops over time by using hyperspectral measurement in NIR to recognize nutrient deficiencies numerous times throughout the growing period. Canonical discriminant analysis was used, and they found a good time to detect chlorophyll reduction in mid and late stages through spectral in red and red edge for N deficiency and senescence period. Many other researchers have studied N and water stress (Pattey et al., 2001, Ferwerda et al., 2005, Feng et al., 2008, Schlemmer et al., 2005, Serrano et al., 2000, Sims and Gamon, 2002).

Vegetation indices are also a good indicator for changes in the physiological and morphological status of plants and whether or not they are stressed (Huete et al., 1994, Qi et al.,

1994). Therefore, spectral vegetation indices SVIs are used wildly in remote sensing applications to verify the conditions of crops (Gilabert et al., 2002). SVIs have helped crop management by providing information about plant pigment, chlorophyll concentration, and water content. Researchers that have studied this technique include (Jackson et al., 2004, Mahlein et al., 2010, Chen et al., 2005, Feng et al., 2012, Anderson et al., 2004). The purpose of this study is to i) select bands that can distinguish between plants that are healthy and those that have laurel wilt, iron deficiency, and nitrogen deficiency in early and late stages of symptom development; ii) detect laurel wilt in avocado trees and utilize a classification method to differentiate between the disease and nutritional deficiencies.

Materials and Methods

Greenhouse Samples

The experiment was carried out at the University of Florida's Tropical Research and Education Center in Miami-Dade County, Florida, near Florida's commercial avocado production area (CAPA). Ten plants were chosen for each treatment, four leaves were collected from each plant, and the trees were one meter high and almost one year old. The experiment had four different treatments, healthy (H), laurel wilt (Lw), iron (Fe), and nitrogen (N) deficiency. To induce laurel wilt symptoms, 10 plants were each inoculated with 3,000 colony forming units (CFUs) of *Raffaelea lauricola*. Four holes were drilled into different sides of each plant's stem with a 7/64" drill bit 5 cm above the graft union, and 25 µL of inoculum prepared with a hem cytometer at a concentration of 30,000 CFUs/mL was pipetted into each hole and wrapped with para film to seal the wound. To induce nutrient deficiencies, 20 avocado trees were transplanted into a nutrient-free matrix (sand and perlite). Half of the plants received 1 L of Hoagland's solution once a week containing all essential nutrients except iron, while the other half received 1 L of Hoagland's solution containing all essential nutrients except nitrogen.

A

Iron deficiency

B

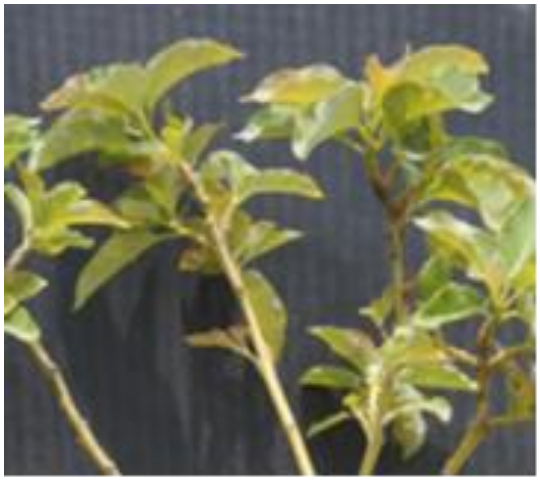

C

Nitrogen deficiency

Healthy plant

Figure 4-1. Leaf pictures of: A) iron deficiency, B) nitrogen deficiency, and healthy plant. Photo courtesy of author, Jaafar Abdulridha

Data Collection

Within the laboratory, spectral data were collected with a spectrometric (SVC HR-1024, Spectra Vista Cooperation, NY) with four fields of view (Figure 1) ranging from 400 to 970 nm, which can be measured with an inexpensive filter. Spectral data were averaged every 10 and 40 nm to normalize the large quantity of spectral data and select bands within these groups, which resulted in 49 and 15 bands, respectively, for the 10 and 40 nm averages. Calibration with a white panel was performed ever 40 scans (Spectral Reflectance Target, CSTM-SRT-99-100, Spectra Vista Cooperation, NY). The spectral data were collected for non-infected, Lw, Fe deficiency, and N deficiency in both laboratory and greenhouse conditions. Two halogen light sources were used to create optimal conditions for performing the scans and reduce errors. The SVC device was situated so that the lens was 50 cm above the sample pointing down at it, and images were taken five times in different positions for each sample. Samples were collected from the Lw plants before external disease symptoms were apparent (Figure 4-2).

Feature Extraction

Selection of spectral reflectance bands and classification, two different feature extraction methods, multilayer perceptron (neural network), and tree decisions were used to select the best bands and classify them at the same time. MLP was used because it was reported to have high accuracy in a previous study by Abdulridha et al. (2016); MLP has high accuracy, therefore was used as decision tree to confirm the result.

Multilayer perceptron is the most common classification method, also known as a supervised network, because it needs output to get results for the desired purpose. The target of this form of the network is to create maps for the input to output in the correct form using the history of the data background. Therefore, it is possible to create the data yield when the chosen yield data is unidentified. A graphical representation of an MLP is shown in Figure 4-2.

The algorithm backpropagation worked repeatedly on all of the data input to the system to frequently represent it in the neural network. With each performance, the yield of the neural network is related to the preferred yield and an error rate is computed. This error rate is fed back to the neural network and used to correct the weight of the data taken, reducing error with each repetition so that the neural network continuously gets closer to creating the preferred yield. The neural network has been applied in remote sensing classification in other studies (Atkinson and Tatnall, 1997, Tzeng et al., 1994, Benediktsson et al., 1990, Heermann and Khazenie, 1992, Foody et al., 1995).

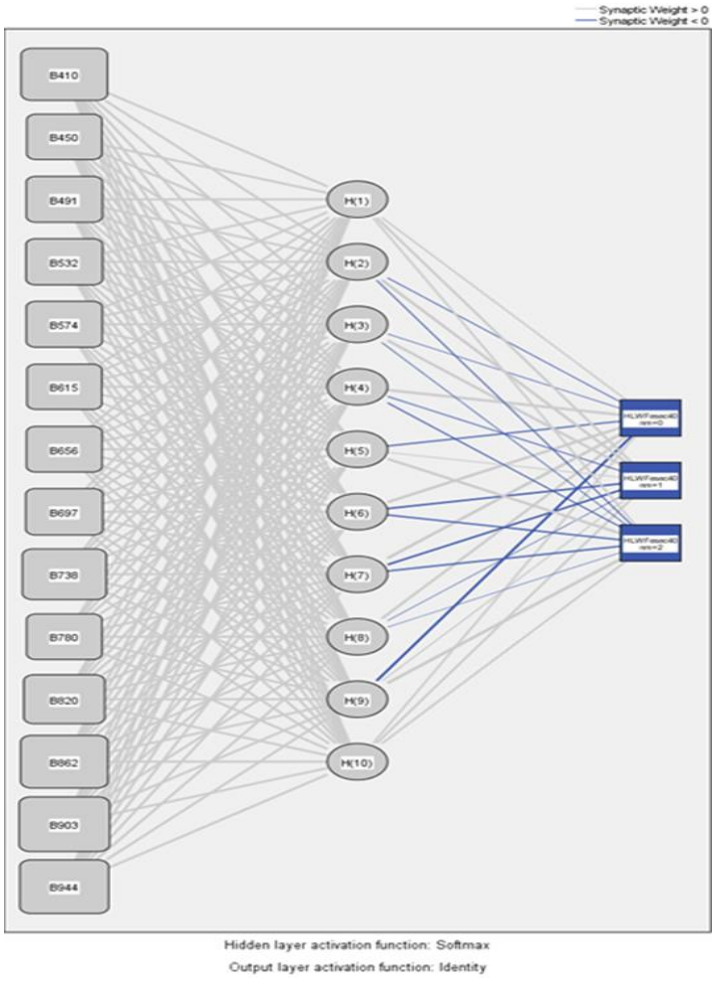

Figure 4-2. Hidden layer and output layer in neural network multilayer perceptron (MLP). Photo courtesy of author, Jaafar Abdulridha

Decision trees (DTs) are a non-parametric managed learning process used for organization and regression. The objective is to produce a model that calculates the value of a goal variable by learning simple choice instructions deducted from data features. DTs are capable of handling data measured on different rulers in the absence of any molds for the proportion distributions of the data individually from the modules, elasticity, and capability to handle non-linear relationships among features and modules (Friedl and Brodley, 1997). Decision trees can be qualified rapidly and are quick in execution. They can be used for feature selection/reduction as well as for organization resolutions. An expert can understand the methods used by a decision tree, and it is not a "black box", like the neural network, which conceals its processes. Decision trees were used for remote sensing data classification in studies by (McIver and Friedl, 2002, Pal and Mather, 2003, Lees and Ritman, 1991).

Two extraction and classification methods were recognized for the spectral wavebands for early and late stages in 10 nm and 40 nm, respectively, for all categories. The best bands were selected and classified to get the highest accuracy to differentiate laurel wilt infested and nutrient deficient plants from healthy controls. In this experiment, 6 bands were selected in high weight values that reached 70% in MLP, and DTs were used to select the most important bands. To get high accuracy, four input ratio methods were used in MLP: training: testing: hold out i) 70%:20%:10%, ii) 60%:30%:10%, iii) 60%:20%:20%, and iv) 80%:10%:10%. Important wavebands were selected from the methods that achieved the highest accuracy.

Vegetation Indices

To compute the vegetation indices for this study, the following waveband ranges were used within the 400-970 nm range: Green (550, 570, 580 nm), red (650, 660 nm), red edge 740 nm, red edge 750 nm, NIR1 761 nm, and NIR2 850 nm (de Castro et al., 2015). Bands were applied to randomize and calculate the vegetation ratio. 23 VIs were applied for H, Lw, Fe, and

N deficiency using ranges from previous literature. The vegetation indices used were: normalize difference vegetation index (NDV1) using 761 nm, and (NDV2) using 850 nm, simple ratio index (SR1) using 761 nm (Rouse et al., 1973), (SR2) using 850 nm, modified triangular vegetation index (MTV 1), (MTV 2) (Ashish, 2013) , renormalize difference vegetation index (Roujean and Breon, 1995), triangular vegetation index (TV 1) (Broge and Leblanc, 2001), modified chlorophyll absorption in reflection index (m CAR) (650, 760, 580 nm) (Haboudane et al., 2004), red-edge vegetation-edge stress index RVS 1, RVS 2 (Merton and Huntington, 1999) green vegetation index VI green (Gitelson et al., 2003), green NDVI (Gitelson and Merzlyak, 1996), structure intensive pigment index (SIPI) (Zarco-Tejada et al., 2000), transformed chlorophyll absorption in reflectance index (TCARI) (Haboudane et al., 2002), photochemical reflectance index (PRI), disease-water stress index 1 (DSWI-1), DSWI-2, water index (WI), ratio of WI and ND, and ND 750/705. VIs give an indicator for pigment and chlorophyll concentration, water stress, and leaf cellular structure using ratios that indicate a high or low amount compared to a non-stressed control plant. After calculating the vegetation ratio, two classifications and selection methods, MLP and DTs, were used to identify the best vegetation indices that could be used to diagnose the Lw and nutrient deficiency.

Results

Wavebands selection: The spectral reflectance displayed distinguishes power. Table 4-1 and 4-2 show the best bands selected in the MLP and DTs classification methods for early and late stages using the 10 nm and 40 nm averages, respectively. In Table 4-1, the classifications were almost 98%, and the most useful bands were selected in visible (VI) (493, 534, 575 nm) Red edge (700-750 nm), and near infrared (NIR) (800-970 nm). In this table, for early and late stage, 10 nm bands were selected between NIR1 and NIR2 (760-850 nm) and MLP classification was 98% and 97%, respectively. The most important bands averaged every 40 nm in early and

late stages were between the visible green band region 900 nm NIR, but the higher values were in visible domain, and for Red edge (534 and 740nm) the weight values were between 78% and 100% for the first 6 bands for early stage 40nm H, Lw, Fe, and N, and the classification was 100%. Additionally, the most significant variables for the late stage 40 nm were between 740 and weighted 100%, and the lower bands in the first 6 bands were 451 nm. Table 4-2 described the decision tree classifications and band selection. Overall accuracy was less than the MLP, between 75% and 85%, and the most common bands were (698, 705, 750 and 822 nm). Abdulridha et al. (2016) (data not published yet) and de Castro et al. (2015) recommended that 700-900 nm was the most important region for distinguishing Lw in avocado trees. In early stages of the disease, it was difficult to recognize spectral reflectance in the visible range, but there was a significant difference in Red edge and NIR (Figure 4-2 A and B). N deficiency had higher reflectance between 700 and 950 nm, while Lw had lower reflectance in this region and had sharp shifting to the NIR domain. In Figure 4-2, spectral bands are exhibited in two different ways. In the VIS and NIR region, N and Fe had almost same reflectance from 540 to 740 nm which peaked above the spectral reflectance of healthy plants. Inverse exhibition was in the NIR region and Lw shifted down in Red edge, after which reflectance increased rapidly in all wavebands. Fe and H had identical curves in Red edge, while N deficiency had lower reflectance in the 740-1340 nm range, after which the reflectance signature increases in the water stress area (970-1450 nm) (Genc et al., 2013, Zygielbaum et al., 2012, Sims and Gamon, 2003, Dobrowski et al., 2005). In both spectral signature curves and band selections, results showed promising bands for the detection of Lw and separating it from the other stress factors.

Vegetation index: Table 4-3 shows the vegetation index for early and late stages used to evaluate the vegetation indices for two classifications MLP and DTs. In early and late stage, the

Table 4-1. Hyperspectral classification and band selection analysis for heathy (H), laurel wilt (Lw), Fe and N deficiency using multilayer perceptron neural network in early and late stage.

Stage and parameters	Important wavelengths (nm)						Over all classification (%)
Early stage 10 nm H, Lw, Fe, N	841	930	750	717	829	739	98
	100%	98%	97%	94%	93%	92%	
Late stage 10 nm H, Lw, Fe N	885	896	874	863	930	852	97
	100%	100%	97%	97%	92%	91%	
Early stage 40 nm H, Lw, Fe, N	534	575	945	822	493	976	98
	100%	95%	95%	92%	86%	78%	
Late stage 40 nm H, Lw, Fe, N	740	781	698	904	863	451	96
	100%	87%	70%	64%	58%	53%	

MLP reported a higher classification from 91%-98% than DTs 80%-82%. Early stage MLP SR 850 was the most important of the vegetation indices, while the lowest was MTVI2 (50%). Late stage ND 750/705, WI, RVS 1, G were the most significant vegetation indices weighted 98% and 61%, respectively. Vegetation indices showed a potential for the detection of Lw and separating it from N and Fe deficiency.

However, spectral reflectance exhibited varied signatures Fe and N exhibited as almost reached same peak value in 540 nm. Lw exhibited different symptoms compared to the early

Table 4-2. Spectral signature analysis (classification and band selection) for H, Lw, Fe, and N deficiency using decision trees in different stages

Stages and parameters	Important wavelengths (nm)	Overall classification (%)
Early stage 10 nm H, Lw, Fe, N	705, 671, 660, 649, 469, 693, 445, 627	80
Late stage 10 nm H, Lw, Fe N	750, 761, 772, 783, 739, 794, 806, 817	82
Early stage 40 nm H, Lw, Fe, N	822, 781, 904, 945, 976, 451, 493, 657	75
Late stage H, Lw, Fe N	698, 617, 493, 575, 451, 410, 534, 781	77

Table 4-3. The important vegetation indices and overall classification in early and late stages. Using multilayer perceptron (MLP) and decision trees (DTs).

Stages and classification methods	Important vegetation indices						Overall Classification (%)
MLP Early stage	SR 850 100%	PRI 94%	NDV850 77%	ND750/705 74%	GNDVI2 68%	mTCARI	98
	SIPI 63%	GNDVI 1 57%	WI 55%	TVI 52%	SIPI 51%	MTVI 2 50%	
MLP Late stage	ND 750/705 100%	WI 85%	RVS 1 64%	G 61%	NDVI 760 58%	GNDVI2 54%	91
	ND 750/660 50%	RDVI 50%					
Decision trees	PRI, Ratio (WI/ND 750/660), ND 750/660, G, VI green, NDVI 760, SR 760, mTCARI, NDV 850						82

stage, with high reflectance in the green and red region up to red edge (Abdulridha et al., 2016 not publish yet). Leaves with Lw symptoms turn yellow, then brown and necrotic in later stages

Discussion

The best band selection and classification methods were described in Table 4-1 and 4-2 for MLP and DTs, respectively, for early stage and late stage in both averages 10 and 40 nm. DTs had lower classifications from 75% to 82%, MLP bands with higher classifications and overall accuracy were used for early stages for 10 and 40 nm band averages, and the classification reached to 98%. The most useful band collected was in the red edge and NIR, where any change in cell structure, leaves pigment concentration, water stress, and cell solution can affect the spectral reflectance (Asrar et al., 1984, Gitelson et al., 2003, Sims and Gamon, 2002) . However, early detection before symptoms appear is important to reduce the economic losses. Disease development will lead to changes in the spectral signature in visible bands or in NIR bands. Within the visible bands, there was no significant difference between H, Lw, Fe, and N deficiency in the late stages of symptom development.

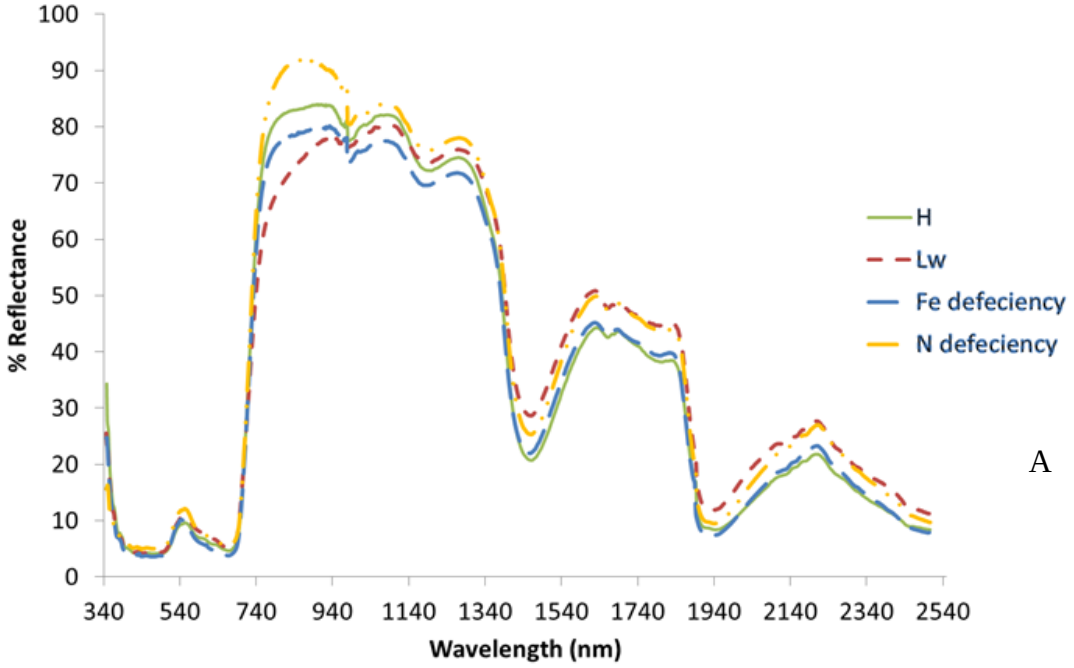

A

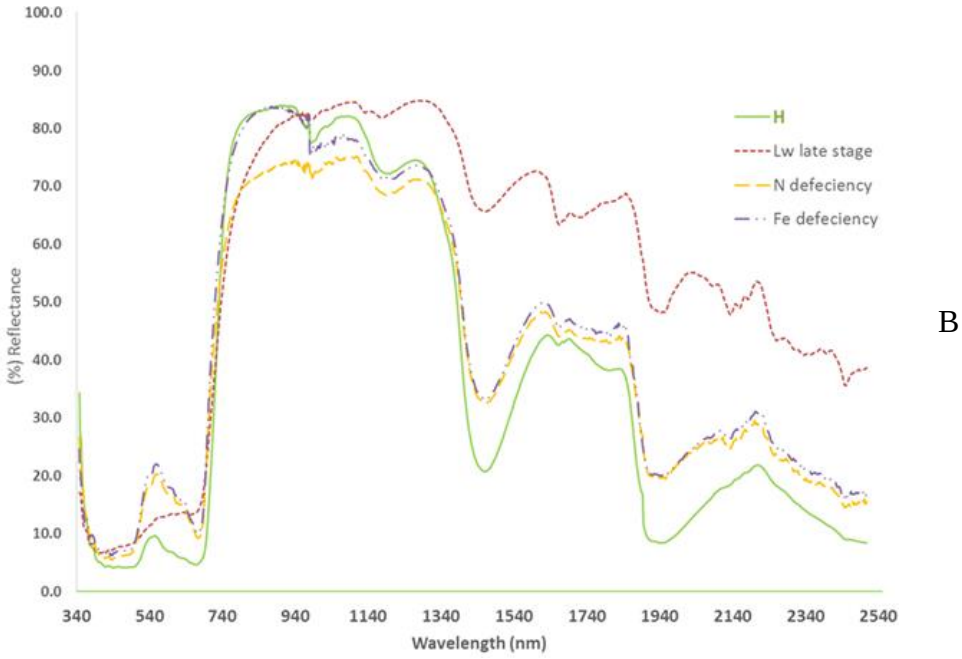

B

Figure 4-3. Spectral signature reflectance of laurel wilt leaves affected with Fe and N deficiency at different disease and nutrient deficiency in indoor conditions. A) Early stress stage and B) advance stress stage.

It was difficult to identify symptoms of Fe and N deficiency within bands in the visible region, but it was possible to detect them in the 740-1000 nm range using NIR. N had higher reflectance than Fe. This is a good indicator that it is possible to monitor nutrient deficiency in early stages (Rodriguez et al., 2006, Alabbas et al., 1974). In late stages, the symptoms of Lw were different from Fe and N deficiency using spectral reflectance, and Lw leaves looked like they were in the senescent stage and had brown spots, while N and Fe turned to yellow, and young leaves turned pale green color. In general, different disease and nutrient deficiencies have the same symptoms in early stages, so it is not possible to confirm symptoms with 100% accuracy unless another method of remote sensing or PCR methods are specially designed for testing large areas. The purpose for determining the 6 bands for use in remote sensing techniques was to detect Lw and classify N and Fe deficiency in the field, so these bands will be used in the field with a camera to cover a large area for aerial imagery. Many other studies have applied this technique to detect diseases and nutrient deficiencies for various crops (Qin et al., 2009, Qin and Zhang, 2005, Prabhakar et al., 2011, Hamed Hamid, 2005). Currently, aerial Lw surveys in Miami-Dade County are visually performed by a surveyor in a helicopter. Each flight is extremely expensive, so unmanned aerial imagery may become a cost-effective solution for identifying trees for removal.

Conclusion

MLP achieved the highest overall classification at 99% for early and late stages, while DTs were less accurate for all treatments. The most important bands selected with the MLP method in early stages for bands averaged every 10 and 40 nm, respectively, were (841, 930, 750, 717, 829, 739), and (534, 575, 945, 822, 493, 976). The wave bands were wide in visible and NIR. Bands with the best values for late stages averaged every 10 and 40 nm, respectively, were (885, 896, 874, 863, 930, and 852) and (740, 781, 698, 904, 863, 451). Almost all of the important bands

were in red edge and near infrared domain. Vegetation indices in the range from 400 to 970 nm were higher for MLP with 92%-98% accuracy for early and late stages compared to the DTs classification of 82%. The vegetation indices selected were (SR 850, PRI) and (ND 750/705, WI) for early and late stage, respectively. In general, spectral signature reflectance and vegetation indices have potential promise for detecting Lw and distinguishing it from other biotic factors.

CHAPTER 5
EVALUATION OF TWO TYPES OF CAMERA TO DISTINGUISH AVOCADO DISEASE AND STRESS FACTORS IN DIFFERENT SEGMENTATION METHODS

Introduction

Avocado is a tropical crop that constitutes a significant economic value in Florida (Evans et al., 2010). In the last few years, Lw infection (produced by the *Raffaela lauricola*) was discovered in avocado (*Persea Americana*) growing regions in south Florida. The avocado production dropped dramatically by 50% as trees were being killed and remaining crops were inferior, low quality, and defective (Evans et al., 2010). Scholars expect avocado industry to collapse in the next few years unless steps are taken to stop the spread of Lw. Laurel wilt is a vascular disease causing high mortality in redbay trees (Mayfield et al., 2008b). The disease is caused by formerly undescribed classes of Raffaelea, a fungal inherent of the non-local redbay invasive insect *Xylebratus glabratus* Eichhoff (Fraedrich et al., 2008, Rabaglia et al., 2006). The first Lw detection was in the United States, near Savannah, GA in 2002. The fungus grew in the avocado trees, causing trees to die in a few weeks (Fraedrich et al., 2008). There are two types of symptoms. One appears on the outer sapwood, as a dark discoloration. The second type appears on the leaves, turning them from oily green to yellow. In the advanced stages, the leaves curl and turn brown (Dreaden et al., 2008, Mayfield et al., 2008a). There are many disease and nutrient deficiencies that show the same symptoms. It is necessary to distinguish Lw from other stressors, to make the right and timely decision to reduce the effect of Lw. Currently, there is no chemical application effective on this disease. Therefore, trees are removed and burned which is the only way to reduce the spread of this disease which has no cure reported to date (Evans et al., 2010). Visually, it is very difficult to recognize Lw from other stress factors, especially in the asymptomatic and early stages, in order to locate a defective tree. There are various methods to diagnose general diseases: a visual method includes ground scouting and aerial surveys.

However, these methods are not accurate, and are expensive not only for avocado crop (Sankaran et al., 2010b, Qin et al., 2009, Qin and Zhang, 2005). Microarray technology (Boonham et al., 2003), DNA, and RNA are both accurate, but time consuming and costly (MacKenzie et al., 1997). The efficiency of ground scouting is difficult. It involves covering large areas from time to time. Many thousands of acres are cultivated in avocado. Futach et al. (2009) studied the efficiency of ground scouting, and they found it was 47% to 61% effective in detecting HLB in citrus orchards but it was time consuming and costly in terms of labor. Rapid identification and removal of Lw-infected trees will decrease the extent of Lw in avocado orchards. Thus, there is a need for new field-based, immediate, and precise detection equipment for improving scouting efficiency to discover disease in orchards (Sankaran et al., 2011). Spectral reflectance from vegetative portions in the short length of visible regions and long wavebands in the near infrared domain of the electromagnetic spectra can be considered as indicator of plant stress (Sankaran et al., 2012, Sankaran and Ehsani, 2012). Many studies have used image processing based on spectral reflectance waveband already selected to recognize healthy plants from non-healthy ones. Moshou (2005) confirmed the possibility of using a multi-band fusion infection detection system, applied in the real-time detection of plant disease in the field. They got satisfactory results after they used a multispectral camera. The overall discrimination error was 11.3% when they discriminated healthy plants, with a yellow rust defective plant. The classification rate between healthy and unhealthy was 94.5% by using quadratic data analysis (Moshou et al., 2004). The target of this study was to moderate the effect of toxic residue levels of pesticide applications and increase the environmental maintenance by studying spectral reflectance between healthy and non-healthy wheat crops (yellow rust). Neural network multilayer perceptrons were used, and the classification rate was 99% higher than Self-Organizing Maps in

early stage. From this result, they could build non-expensive remote sensors to apply in the field. Muhammed (2005) studied how the spectral signature worked with disease severity, and confirmed that development stage could change the reflectance signature and normalization values. The best classification result was obtained by using nearest-neighbor method. Camargo and Smith (2009a) found methods in image processing to convert RGB images of the diseased plant or leaf into the H, I3a, and I3b color transformations. Neighborhood classification methods were used for each pixel and the gradient of variation between them (Camargo and Smith, 2009b). Examinations showed the performance of colored images by using a support vector machine (SVM) classifier, and examinations of diseases in cotton crop regions were exposed in digital images. Nilsson (1995) emphasized that spectral image application would increase correctness and precision application in order to obtain a high level of accuracy to reduce disease damage. Qin and Zhang (2005) demonstrated that a hyperspectral imaging technique coupled with the spectral information divergence (SID) classification method, based on the image organization process, could be used for discriminating citrus canker from other confounding citrus pathogens. The classification accuracy was 96%. Balasundaram (2009) classified canker citrus peel and the severity of development disease stage. They pursued different citrus varieties. A spectrophotometer, with a wavelength range of 200-2500 nm, was used to measure the spectral reflectance data of citrus peel. The result of discriminant classification was 98%. A hyperspectral camera of 369-1042 nm was employed to attain hyperspectral pictures of green fruits of multiple citrus varieties. Linear discriminant analysis was used to classify different citrus varieties. The classification values varied depending on variety by 70-85% (Okamoto and Lee, 2009). A thermal and a visible sensor of a citrus canopy were combined to improve fruit detection. Two image fusion methods were tested: the Laplacian pyramid transform (LPT) and fuzzy logic.

Both image fusion approaches enhanced fruit detection when related to use the thermal image individually (Bulanon et al., 2009). Lewis et al.(2001) recognized different types of vegetation canopies by using hyperspectral imagery in a semi-arid climate, and found that it was possible to use short wave and near infrared spectral reflectance technology. In the short wavebands infrared cellulose–lignin had highest absorption amount than in narrow bands because of the availability of wax and oil in the leaves. There is another study which focused on the comparison between image analysis and stereomicroscope for fruit trials. Fruit shape, fruit length, and fruit size were used as parameters to compare both methods. It was found there are no significant differences between the two methods; therefore, image analysis was recommended to save time, labor, and reduce human error (Mix et al., 2003). The fruit industry also considered the benefit of image processing to classify good fruit from defective fruit. Ariana et al.(2006) utilized image analysis to recognize multiple varieties and multiple fruit properties standard, black rot, decline, soft burn, and superficial scald tissues. Artificial neural network organization models were established, and the method is capable of accurate recognition of diverse types of disorders on apples. The present study evaluated the application of two types of cameras in different band filters selected and different development disease stages between healthy and Lw and classified H, Lw, Prr, Fe, and N deficiency in two regions of interest: the polygon region of interest (PROI) and the overall region of interest (OVRI) in the asymptomatic stage (Asy) and symptomatic stage (Sym).

Material and Methods

Study Zone

The affected wavebands were selected in previous studies after spectral analysis were done in lab conditions. The images were taken and analyzed at the Citrus Research and Education Center (CREC), Lake Alfred, University of Florida (latitude and longitude coordinates

28.101880°, - 1.713923). Figure 1 shows a regular picture (RGB) from a Sony camera. There were five classes needed to be classified. Tree pots were distributed randomly in a rectangular area (6 m × 4.20 m) to make sure they were in the same light conditions and vegetation density. Avocado trees were grown and inoculated in greenhouses at the Tropical Research and Education Center, University of Florida, Homestead. Ten trees were inoculated with Lw *R. lauricola* by applying it into four holes that were drilled into the tree trunk. Each hole was filled in 750 conidia of the fungus. The total amount was 3,000 per plant. Holes were sealed with paraffin wrap. After 10 days, symptoms began, and some leaves started to turn yellow. After 24 days, the leaf color changed to brown. In reference to Phytophthora root rot (Prr), 10 plants were injected with 6 grams of wheat seeds populated with Prr cinnamomi. After 60 days, captured images for these plants showed a decline.

Nutrient Deficiency

Twenty avocado trees were transplanted into a non-nutrient matrix (sand and perlite). Half of the plants received Hoagland's solution with complete nutrients except iron, and the other half were given complete nutrient except for nitrogen. Images were captured after two years. Spectral reflectance measurements were taken and explained in previous chapters. Spectral reflectance data were collected under controlled laboratory conditions at the Tropical Research and Education Center, University of Florida (TREC) with a handheld spectrodiometer (SVC HR-1024 spectrodiometer, Spectra Vista Corporation at 50 cm height above each leaf with a 4º field-of-view optical lens in the spectral range of 350 to 2500 nm.

Image Acquisition

Two different types of cameras were used in order to evaluate and select the best camera to classify healthy from stressed plants. A Hi-lift machine was used in this study to collect images from different altitude levels (Figure 1). Altitude was 25 ft for Canon, and 32 ft for tetra Cam.

Camera filters were chosen from a previous study. More than six bands were selected as high weight value (Abdulridha et al., 2016, data not published yet).

Data Field

The images were taken in sunny conditions from 11:00 a.m. to 2:00 p.m. Trees were in pots, so we could move them (Figure 2). Avocado trees were in different stress stages to study the ability to detect Lw disease in more than one stage: in the asymptomatic stage (Asy stage), 70% of the leaves looks green; however, we could see some leaves turning yellow in spots. Second stages were late, and in intermediate or symptomatic stage (Sym stage), some leaves dehydrated and turned from yellow to curly brown. The trees died in short time, and about one month later, all trees were dried and brittle. In the Asy stage, each tree position was considered as a region of interest and calculated individually. Data were saved in an Excel file.

Types of Cameras

There were two types of cameras chosen in order to capture images to the canopy region after selecting the discriminate wavebands:

Tetra cam mini: (Tetra cam, Inc., CA, USA) multispectral camera with six individual digital sensors MCA- 6 arranged in a 3 × 2 array, independent optics and user customizable band pass filters (Andover Corporation, NH, USA). Each unit holds a 1.3 megapixel CMOS sensor (1,280 × 1,024 pixels), FOV of 43.7º × 35.6º, central length of 9.6 mm. Images are saved in independent solid flash cards integral in the camera with 8-bit radiometric purpose. Multispectral images were taken in this camera (Green, G: 580-10 nm; Red, R650: 650-10 nm, Red-edge, Redge740: 740-10 nm, Red-edge, Redge750: 750-10 nm, NIR, NIR760: 760-10 nm, NIR, NIR850: 850-40 nm) images were captured from a Hi-lift on April 10 and 24, 2015.

Modified Canon (CanonSX260 NDVI, Canon U.S.A., Inc. Melville, NY, USA) 37 mm filter ring was added above the front lanes of the camera. This was done by manufactory-made

A 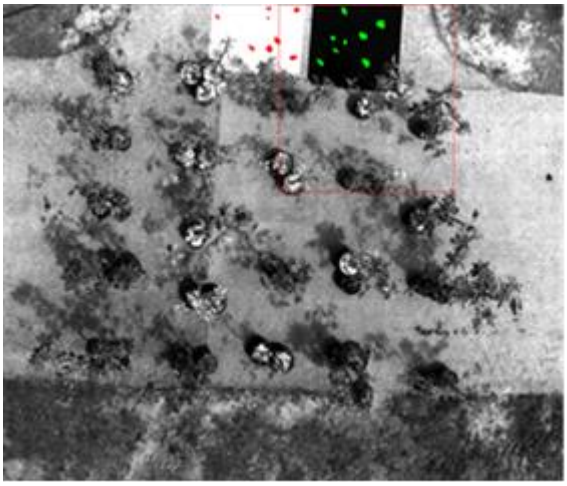  B

Figure 5-1. Images were taken by canon camera. A) RGB Image captured on regular camera. B) Canon image captured. Photos courtesy of author, Jaafar Abdulridha

(LDP-LLC, Carlstadt, NJ 07072 USA); all images were kept on a digital memory card. The purpose of adding this filter was to capture data in the visible range (green and blue) and red edge (R mod GB: blue, B:390-520 nm; green, G: 470-570 nm; red-edge, Rmod:670-750 nm) (de Castro et al., 2015). Calibrations were accrued in the field with a white and black panel. This typically is able of obtaining 12.1 mega pixel spatial resolution images with 8-bit radiometric resolution and is fitted out with a 5.7-18.8 mm zoom lens.

Image Pre-Processing

Multiband images need to apply an alignment process to reduce the interaction between bands and make identical lines for six images. Canon images do not need alignment. Pixel Wrench (PW2) software (Tetracam Inc., Chatsworth, CA, USA) was utilized for this purpose. Bands were built up in individual band channel in each shoot. Viola and Wells (1997) recommended applying alignment to multispectral images in order to obtain high resolution by making each band image identical for each other's images in one shoot. This is referred to as image rectification (Cheng et al., 2000). Images had been taken in real coordinates (Vanwie and Stein, 1977). Field-of-view (FOV) optical vignette parameters were considered and adjusted in

ideal methods. Radiometric rectification was accrued by using two calibration sheets, black and white (1.2×1.2m; Group 8 Technology, Inc., UT, USA). The average for black and white were calculated and each reflectance pixel was computed based on these averages (Chang and Reid, 1996, Schott et al., 1988). ENVI software (ENVI, Research Systems Inc., Boulder, CO, USA) was utilized to integrate six images. ROI also was selected in polygon and overall ROI (Figure 5-2), then exported ROI from text file to an Excel file to process reflectance data to be in SPSS format. Pixel-based retrieved reflectance data were mixed together for each class to reduce the illumination variability and light incident. In PROI, data were selected from the leaf center to avoid any interaction between classes as well (Figure 5-2 B). Data were calibrated and run in two classification methods: neural network multilayer perceptron (MLP) and K-nearest neighbor (KNN).

A 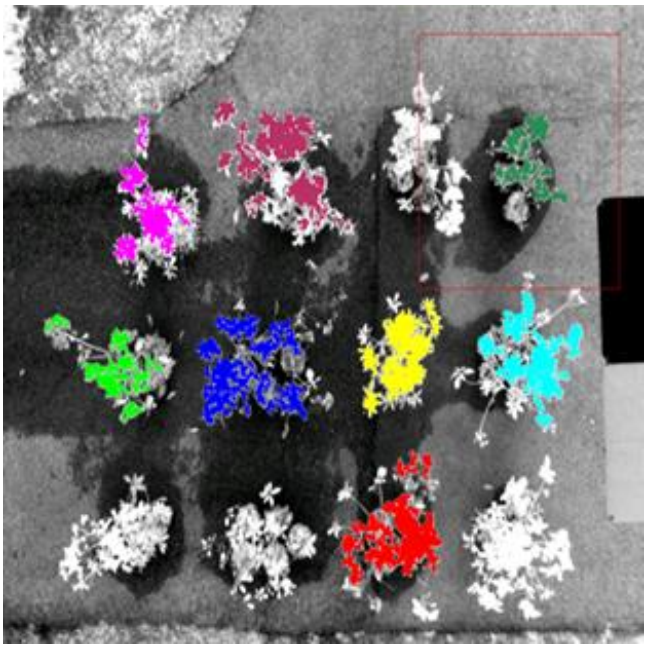 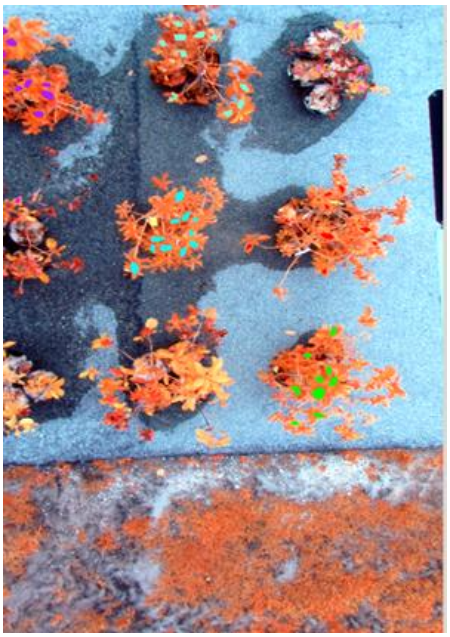 B

Figure 5-2. Overall and polygon region of interest were taken by tetra camera. A) Overall region of interest. B) Image of polygon region of interest Photo courtesy of author, Jaafar Abdulridha

Data Analysis

SPSS software (SPSS 13.0, Inc., Chicago; Microsoft Corp., Redmond, WA) was utilized in this study for spectral analysis. Two different feature extraction methods, (MLP) (neural network), and (KNN) were used to select best bands and classify in same time. From a previous study (Abdulridha et al., 2015a), it was found that MLP has high accuracy; therefore, KNN was used to confirm the results.

Multilayer perceptron

Multilayer perceptron is the most common classification method, also known as a supervised network, because it needs output to get results in the desired purpose. The target of this form of the network: to create maps for the input and output in correct ways, using historical data background. Therefore, it is possible to create the data yield when the chosen yield data is unidentified. There is an algorithm called backpropagation that works on all the input data in the system to present input data frequently in neural network. With each performance, the yield of the neural network is related to the preferred yield and a miscalculation is computed. This inaccuracy is the feedback to the neural network and used to correct the weight; therefore, the error reduces with each repetition and the neural typical gets very close to creating preferred yield. Neural network has been applied in remote sensing classification (Serpico et al., 1996, Atkinson and Tatnall, 1997, Benediktsson et al., 1990, Foody et al., 1995, Tzeng et al., 1994).

Nearest neighbor

An un-dimensional method, the distance between correlation coefficient and sum of squared variance are given good indicators to the strength recognition or weakness recognition of two spectral vectors. The best way to examine the relationship between two pixel points is to find out the correlation coefficient estimated from equation (1) in which the distance vector mean considered as the interior item of two vectors divided by N. This leads to use a much simpler

portion, symbolized by s, which is just the inner item of the two vectors, considering that the "vectors must be whitened" (Pydipati et al., 2006, Foody et al., 1995). Clearly, it is relative to the other distance quantity as defined in equation (2). The calculated distances are then used to find the k training models that are nearby to the unknown model based on these nearest neighbors. The purpose of classification is recognition between different categories. A more advance tactic used in this study was to give a diverse weight to the contribution of each of the K-nearest neighbors in the estimation.

$$R = \frac{\sum_{i=1}^{N}(X1(i) - \overline{X1})(X2(i) - \overline{X2})}{\sqrt{\sum_{i=1}^{N}(X1(i) - \overline{X1})^2 \sum_{i=1}^{N}(X2(i) - \overline{X2})^2}} \quad (1)$$

$$\sum_{i=1}^{N} \left(X1(i) - X2(i)\right)^2 \quad \textbf{(2)}$$

N: Distance vector

$\overline{X1}$, $\overline{X2}$: mean of $X1$ and X2

Image Classification Methods

The classification was between healthy plant-control (H), laurel wilt disease (Lw), Phytophthora root rot disease (Prr), and N and Fe deficiency. The images were taken for two Lw stages in the Asy stage and in the Sym stage, and in two different regions of interest: polygon region of interest (PROI) and overall region of interest (OVROI). For polygon ROI, only eight leaves were selected randomly from all over the plant, including tree branches. The classification was done between H vs. Lw, H vs. all factors (Lw, Prr, N, Fe) and Lw vs. (H, Prr, N, Fe). Table 5-1 shows pixel numbers for the polygon and the overall region of interest. Obviously, the

polygon regions of interest (PROI) had pixel numbers less than the overall region of interest the pixel number in last one reached many thousands.

The other classification was between three categories: H vs. Lw vs. Prr, H vs. Lw vs. N, H vs. Lw vs. Fe and all categories together H vs. Lw vs. Prr vs. N vs. Fe.

Results and Discussion

Pixel cell numbers show how much area is captured from the tree canopy (Pohl and van Genderen, 1998). For each class, from Table 5-1 it is obvious that OVROI has larger pixel numbers than PROI. To determine pixel numbers for each plant, canopy size matters from upper view. Thus, choosing pixel position is critical to get high resolution and reduce background subtraction for the image (Zivkovic and van der Heijden, 2006, Yamaguchi et al., 2001). However canopy density with other factors such as sunlight, camera angle, water evaporation, could affect image resolution (Holben, 1986). Pixel number parameters are considered when capturing remote images. These parameters have a significant effect in spatial resolution, coverage zone area, time and cost effectiveness, and spectral resolution (Kingsbury, 1999).

Table 5-1. Number of pixels for two types of camera: Canon cam (3 bands), Tetra cam (6 bands) and include all classes (healthy, Lw, Prr, N, Fe, and white-black panel) for both region of interest polygon and overall ROI

Classes	Canon Cam (3 bands)		Tetra cam (6 bands)	
	Polygon ROI	Overall ROI	Polygon ROI	Overall ROI
White panel	1,399	46,515	1,824	31,380
Black panel	1,317	48,954	1,740	14,832
H	1,458	25,674	1,569	5,020
Lw	3,450	70,305	2,372	14,494
Prr	3,100	33,002	2,086	9,203
N	1,758	18,355	1,702	4,419
Fe	2,830	42,639	2,372	10,382

Table 5-2. The comparison of two types of camera Canon (3 bands), and tetra cam (6 bands) by using two classification methods: multilayer perceptron neural network MLP and K-nearest neighbor with PROI in Sym and Asym stages.

Classes in asymptomatic	Canon camera		Tetra camera	
stage polygon ROI	MLP (%)	KNN (%)	MLP (%)	KNN (%)
H&Lw	73	63	80	73
H&Fe	71	66	95	82
H&N	84	77	99	88
H&Prr	72	66	83	76
H& other factors	86	53	82	68
Lw& other factors	73	70	78	76
Classes in symptomatic stage				
H&Lw	76	63	83	73
H& other factors	87	68	92	79
Lw& other factors	75	68	82	70

Table 5-3. The comparison of a classification accuracy two types of camera Canon (3 bands), and tetra cam (6 bands) by using two classifications: multilayer perceptron neural network and K-nearest neighbor OVROI in Sym and Asym stage.

Classes in asymptomatic stage over	Canon cam		Tetra cam	
all plant ROI	MLP (%)	KNN (%)	MLP (%)	KNN (%)
H&Lw	76	63	85	82
H&Fe	69	58	91	82
H&N	74	68	98	89
H&Prr	62	58	86	75
H& other factors	87	80	83	67
Lw& other factors	77	73	79	74
Classes in symptomatic stage				
H&Lw	78	68	86	72
H& other factors	88	67	93	77
Lw& other factors	77	70	83	68

Table 5-4. The classification accuracy between healthy, laurel wilt, Fe, N, and Phytophthora root rot by using two classification methods (MLP and KNN) for two stages, and two cameras Canon (3 bands) and Tetra cam (6 bands).

Classes in Asymptomatic stage	Canon camera		Tetra cam	
	MLP (%)	KNN (%)	MLP (%)	KNN (%)
H-Lw-Fe	57	52	77	73
H-Lw-N	65	51	75	72
H-Lw-Prr	55	55	74	61
H-Lw-Fe-N-Prr	43	40	53	48
Classes in Symptomatic stage				
H-Lw-Fe	67	58	83	50
H-Lw-N	70	60	86	52
H-Lw-Prr	67	62	81	51
H-Lw-Fe-N-Prr	60	56	65	58

PROI-Asy Stage: From Table 5-2 the result of PROI Tetra cam (6 bands) shows high classification value to discriminate H vs. Lw in MLP classification method, while Canon 3 bands were higher than other camera to distinguish Lw from other factors (H, Fe, N, and Prr). When the leaves of avocado were infected with ambrosia beetle and caused Lw, this beetle produced fungal distract water flow to leaves (Ploetz et al., 2012a). Eventually, leaves turned a different color, so spectral reflectance was affected in near infrared region. Any change in leaf color and leaf structure is an indicator that there is stress on leaves and will effect spectral reflectance.

PROI - Sym stage: The filter of tetra camera was included six bands 580-10 nm, 650-10 nm, 740-10 nm, 750-10 nm, 760-10 nm, and 850-40 323 nm had higher classification than other cameras. The classification value of H and other factors has higher value than other camera and for both ROI and both stages. The higher classification between healthy and other factors included Lw in Asy and Sym stages. KNN has lower classification than MLP in all treatments,

so we focused on the MLP method. The situation of non-infected leaves has high chlorophyll concentration, the reflectance range of chlorophyll content 520-550 nm and 695-705 nm of all species (Gitelson et al., 2003). In the visible range, light was absorbed in blue and red range, while it reflects green color in green region 520-550 nm (Penuelas et al., 1995, Chappelle et al., 1992). Any change in chlorophyll content will lead to change in leaves spectral reflectance in visible range (Sims and Gamon, 2002). The disease development stage might affect reflectance value in visible and near infrared (NIR) domain (Sims and Gamon, 2002). When the Lw disease started to develop in avocado trees, leaves dramatically changed from green to yellow, then turned to wilt brown. Finally, the leaves dried and were totally necrotic. The severity of the disease dramatically changes leaf structure and water content depends on disease development stages (Chappelle et al., 1992).

OVROI - Sym: From Table 5-3: The Canon cam had lower classification value for both MLP and KNN. H vs. N recorded as higher classification value could be distinguished between healthy and N deficiency. In general, the good classification belonged to tetra cam 6 bands. The higher classification value between two classes H vs. N, H vs. Fe; the classification reached up to 98% in some cases. As was mentioned above, there were two types of filters and cameras used to distinguish H and other stress factors. Obviously, the tetra cam 6 bands was the best filter to discriminate different classes in high classification value than other camera and filter.

In image processing, wavelets might be used for multi-resolution images. Filter selection is important to provide good resolution separable between wavelengths (Kingsbury, 1999). Splitting infected trees from un-infected in remote sensing is critical in order to distinguish various stresses in a plant, so eliminating any interaction between specific wavelengths that will reduce or eliminate any image analysis confusion. However, band filter selection affects the

result of classification. More band selections will lead to higher resolution and more separation between different classes depending on precision of band selection to reduce any interaction between narrow wavelengths (Chang et al., 1999). From the result, filter coefficient effect classification result (Villasenor et al., 1995), we could prove that wavebands were already selected in lab condition.

Conclusion

Image processing with optimal band selection is more effective in recognizing infected plants from non-infected plants. In this study, two cameras with different filters and different bands selection were utilized to evaluate the performance of these cameras (MCA tetra cam-6, Tetra cam, and Canon-3 bands). For evaluation, two classification methods (MLP and KNN) were implemented. In addition, two regions of interest (PROI and OVROI) were applied to figure out which segmentation could work. Categories of avocado trees were classified (H, Lw, Prr, Fe, and N) in two Lw stages, early and late stage. MLP method was better than KNN in all treatments, and in some cases reached up to 98%. OVROI had higher classification and higher resolution and larger pixel numbers than PROI. The Canon cam recorded less classification value than MCA tetra cam. In general, tetra cam 6 bands (580-10 nm, 650-10 nm, 740-10 nm, 750-10 nm, 760-10 nm, and 850-40 323 nm) had the highest classification for most treatments. Lw Sym stage recorded higher classification than the Asy stage. The classification of H and (Lw, Prr, Fe, and N) Fe and N deficiency had higher recognition value in most treatments for all cameras and OVROI. The quality of filter bands selection is critical in remote sensing to provide accurate spectral reflectance. It will give good results in distinguishing healthy plants from non-healthy ones. Inexpensive remote sensing could encourage growers to use image application as a nondestructive method to detect biological and non-biological factors in groves with low cost and accurate method.

CHAPTER 6
SUMMARY AND RECOMMENDATIONS

The main target of this study was to find out inexpensive remote sensing technique to detect Lw infected trees. In this study, spectral reflectance was measured for canopy of healthy (control), Lw infected, Prr infected, salinity damage, Fe and N deficiency using SVC HR-1024 portable spectrodiometer (Spectra Vista Corporation, Poughkeepsie, New York), Tetra cam 6 bands (Tetra cam, Inc., CA, USA), and Modified Canon (CanonSX260 NDVI, Canon U.S.A., Inc. Melville, NY, USA). Five classification algorithm methods such as neural network multilayer perceptron (MLP) and radial base function RBF), step wise discriminant analysis (STEPDISC), decision tree (DT) and K-nearest neighbor (KNN) were applied. These images were processed in ENVI 4.5 (ITT Visual Information Solutions, Boulder, Colorado).

Chapter One: Review of benefit of remote sensing technique, and overview of principle of remote sensor description of disease detection technique improvement through several studies had done. Discuss disease detection methods and focusing on non-distractive method and show the importance of spectral reflectance method and hyperspectral and multispectral image and explain how it is environmental friendly and inexpensive comparing to DNA analysis.

Chapter Two: Describes the brief overview of all suspected diseases similar to Lw and nutrient deficiencies that may be confused with Lw. Mention the most important factors affect spectral reflectance and absorbance in leaf area such as chlorophyll concentration, leaf structure, and water content. This chapter also describes the mechanism of Lw and effect on commercial avocado area in south Florida. It also discusses the diseases in avocado caused by vectors, virus, pathogens, and the symptoms of multi-mineral deficiency have the same early symptoms with Lw.

Chapter Three: Two neural network MLP and RBF and STEPDISC classification methods to identify the ability of discrimination of Lw, control, Prr, and salinity damage in early and late stage. The result was almost perfect discrimination between all treatments. MLP method was the best distinguish for all classification method reach up to 98%. The most important bands were between red and NIR domain. The results also show it is possible to detect disease before disease symptom appearances.

Chapter Four: Discuss the effect of Lw and nutrient deficiency, and capability of detecting the disease in MLP and decision tree (DT) algorithm classification were used to identify Lw and Fe and N deficiency using a Spectra Vista spectrodiometer. The result showed the possibility to identify Lw from H, N, and Fe deficiency in early symptomatic. MLP has highest classification rate reached up to 98%. Almost all of the important bands were in red edge and near infrared domain. Vegetation indices in the range from 400 to 970 nm were higher for MLP with 92%-98% accuracy for early and late stages compared to the DTs classification of 82%. The vegetation indices selected were (SR 850, PRI) and (ND 750/705, WI) for early and late stage, respectively.

Chapter Five: Applied two different cameras: Tetracam 6 bands and Canon red modify to detect Lw in a symptom and in advance symptomatic stage with H, Prr, N, and Fe deficiency. MLP and KNN algorithm methods were used to classify multiband spectral reflectance for two region of interest polygon and overall region of interest included all canopy of tree while (PROI) covered just leaves partially (segmentation); however, the good results we obtained Tetra cam 6 bands - MLP classification method with (OVROI) in some treatment reached up to 99% especially for healthy and N. From image analysis, it was clear and possible to recognize trees

under stress and non-infected trees with high accuracy, so multiband image with good bands selected for sure would give good result in precision agriculture.

High accuracy of spectral bands selection is essential to use these bands in camera's filter in order to detect stress factors and distinguish it with high accuracy. The application of this study used in limited area and samples. Therefore, it is necessary to apply this technique in real field with multi stress factors.

LIST OF REFERENCES

ABADIA, J., MORALES, F. & ABADIA, A. (1999) Photosystem II efficiency in low chlorophyll, iron-deficient leaves. *Plant and Soil,* **215,** 183-192.

AHRENS, U. & SEEMULLER, E. (1992) Detection of dna of plant pathogenic mycoplasmalikeorganisms by a polymerase chain-reaction that amplifies a sequence of the 16s rna gene. *Phytopathology,* **82,** 828-832.

ALABBAS, A. H., BARR, R., HALL, J. D., CRANE, F. L. & BAUMGARD.MF (1974) Spectra of normal and nutrient-deficient maize leaves. *Agronomy Journal,* **66,** 16-20.

ALLEN, W. A. & ROBERTS, J. E., SR. (1974) Economic feasibility of scouting soybean insects in late summer in Virginia. *Journal of Economic Entomology,* **67,** 644-647.

ANDERSON, M. C., NEALE, C. M. U., LI, F., NORMAN, J. M., KUSTAS, W. P., JAYANTHI, H. & CHAVEZ, J. (2004) Upscaling ground observations of vegetation water content, canopy height, and leaf area index during SMEX02 using aircraft and Landsat imagery. *Remote Sensing of Environment,* **92,** 447-464.

APAN, A., HELD, A., PHINN, S. & MARKLEY, J. (2004) Detecting sugarcane 'orange rust' disease using EO-1 Hyperion hyperspectral imagery. *International Journal of Remote Sensing,* **25,** 489-498.

ARIANA, D., GUYER, D. E. & SHRESTHA, B. (2006) Integrating multispectral reflectance and fluorescence imaging for defect detection on apples. *Computers and Electronics in Agriculture,* **50,** 148-161.

ASHISH, R. M. (2013) Early detection of citrus greening (HLB) using ground based hyperspectral imaging and spectroscopy. In: *ABE*. University of Florida.

ASRAR, G., FUCHS, M., KANEMASU, E. T. & HATFIELD, J. L. (1984) Estimating absorbed photosynthetic radiation and leaf-area index from spectral reflectance in wheat. *Agronomy Journal,* **76,** 300-306.

ATKINSON, P. M. & TATNALL, A. R. L. (1997) Neural networks in remote sensing - Introduction. *International Journal of Remote Sensing,* **18,** 699-709.

AYALA-SILVA, T., GORDON, G. G., SCHNELL, R. & WINTERSTEIN, M. (2012) Application of propiconazole in management of laurel wilt disease in avocado (persea americana Mill.) trees. *Acta Horticulturae,* 71-78.

AYERS, A. D., ALDRICH, D. G. & COONY, J. J. (1952) Sodium and chloride injury of Fuerte avocado leaves. *Yearbook of the California Avocado Society for the year 1951,* 174-178.

BALASUNDARAM, D., BURKS, T. F., BULANON, D. M., SCHUBERT, T. & LEE, W. S. (2009) Spectral reflectance characteristics of citrus canker and other peel conditions of grapefruit. *Postharvest Biology and Technology,* **51,** 220-226.

BAR, Y., APELBAUM, A., KAFKAFI, U. & GOREN, R. (1997) Relationship between chloride and nitrate and its effect on growth and mineral composition of avocado and citrus plants. *Journal of Plant Nutrition,* **20,** 715-731.

BARANOSKI, G. V. G. & ROKNE, J. G. (2005) A practical approach for estimating the red edge position of plant leaf reflectance. *International Journal of Remote Sensing,* **26,** 503-521.

BARNARD, R. O., CILLIE, G. E. B. & KOTZE, J. M. (1991) Deficiency symptoms in avocados. *Yearbook - South African Avocado Growers' Association,* **14,** 67-71.

BARRETT, E. C. & CURTIS, L. F. (1999) *Introduction to environmental remote sensing*.

BATES, C. A., FRAEDRICH, S. W., HARRINGTON, T. C., CAMERON, R. S., MENARD, R. D. & BEST, G. S. (2013) First report of laurel wilt, caused by *Raffaelea lauricola,* on sassafras (sassafras Albidum) in Alabama. *Plant Disease,* **97,** 688-688.

BAURIEGEL, E., GIEBEL, A., GEYER, M., SCHMIDT, U. & HERPPICH, W. B. (2011) Early detection of Fusarium infection in wheat using hyper-spectral imaging. *Computers and Electronics in Agriculture,* **75,** 304-312.

BENEDIKTSSON, J. A., SWAIN, P. H. & ERSOY, O. K. (1990) Neural network approaches versus statistical-methods in classification of multisource remote-sensing data. *Ieee Transactions on Geoscience and Remote Sensing,* **28,** 540-552.

BERNAL, M., CASES, R., PICOREL, R. & YRUELA, I. (2007) Foliar and root Cu supply affect differently Fe- and Zn-uptake and photosynthetic activity in soybean plants. *Environmental and Experimental Botany,* **60,** 145-150.

BERNSTEIN, L. (1975) *Effects of salinity and sodicity on plant growth*.

BHATTI, A. S. & LONERAGAN, J. F. (1970) Phosphorus concentrations in wheat leaves in relation to phosphorus toxicity. *Agronomy Journal,* **62,** 288-290.

BLACKBURN, G. A. (1998) Spectral indices for estimating photosynthetic pigment concentrations: a test using senescent tree leaves. *International Journal of Remote Sensing,* **19,** 657-675.

BOONHAM, N., WALSH, K., SMITH, P., MADAGAN, K., GRAHAM, I. & BARKER, I. (2003) Detection of potato viruses using microarray technology: towards a generic method for plant viral disease diagnosis. *Journal of Virological Methods,* **108,** 181-187.

BOROUJERDNIA, M., ANSARI, N. A. & DEHCORDIE, F. S. (2007) Effect of cultivars, harvesting time and level of nitrogen fertilizer on nitrate and nitrite content, yield in romaine lettuce. *Asian Journal of Plant Sciences,* **6,** 550-553.

BRAVO, C., MOSHOU, D., WEST, J., MCCARTNEY, A. & RAMON, H. (2003) Early disease detection in wheat fields using spectral reflectance. *Biosystems Engineering,* **84,** 137-145.

BROGE, N. H. & LEBLANC, E. (2001) Comparing prediction power and stability of broadband and hyperspectral vegetation indices for estimation of green leaf area index and canopy chlorophyll density. *Remote Sensing of Environment,* **76,** 156-172.

BULANON, D. M., BURKS, T. F. & ALCHANATIS, V. (2009) Image fusion of visible and thermal images for fruit detection. *Biosystems Engineering,* **103,** 12-22.

BURGESS, M. W. (1983) Development of cotton-pest management in Zimbabwe. *Crop Protection,* **2,** 247-250.

BURKS, T. F., SHEARER, S. A., HEATH, J. R. & DONOHUE, K. D. (2005) Evaluation of neural-network classifiers for weed species discrimination. *Biosystems Engineering,* **91,** 293-304.

CAKMAK, I., HENGELER, C. & MARSCHNER, H. (1994) Change in phloem export of scurose in leaves in response to phosphorus, potassium and magnesium-deficiency in bean-plants. *Journal of Experimental Botany,* **45,** 1251-1257.

CAMARGO, A. & SMITH, J. S. (2009a) An image-processing based algorithm to automatically identify plant disease visual symptoms. *Biosystems Engineering,* **102,** 9-21.

CAMARGO, A. & SMITH, J. S. (2009b) Image pattern classification for the identification of disease causing agents in plants. *Computers and Electronics in Agriculture,* **66,** 121-125.

CAMPS, C. & CHRISTEN, D. (2009) Non-destructive assessment of apricot fruit quality by portable visible-near infrared spectroscopy. *Lwt-Food Science and Technology,* **42,** 1125-1131.

CARRERO, P., MALAVE, A., ROJAS, E., RONDON, C., DE PENA, Y. P., BURGUERA, J. L. & BURGUERA, M. (2005) On-line generation and hydrolysis of methyl borate for the spectrophotometric determination of boron in soil and plants with azomethine-H. *Talanta,* **68,** 374-381.

CARRILLO, D., CRANE, J. H. & PENA, J. E. (2013) Potential of contact insecticides to control Xyleborus glabratus (Coleoptera: Curculionidae), a vector of laurel wilt disease in avocados. *Journal of Economic Entomology,* **106,** 2286-2295.

CARRILLO, D., DUNCAN, R. E. & PENA, J. E. (2012) Ambrosia beetles (coleoptera: curculionidae: scolytinae) that breed in avocado wood in florida. *Florida Entomologist,* **95,** 573-579.

CARTER, G. A. & KNAPP, A. K. (2001) Leaf optical properties in higher plants: Linking spectral characteristics to stress and chlorophyll concentration. *American Journal of Botany,* **88,** 677-684.

CECCATO, P., FLASSE, S., TARANTOLA, S., JACQUEMOUD, S. & GREGOIRE, J. M. (2001) Detecting vegetation leaf water content using reflectance in the optical domain. *Remote Sensing of Environment,* **77,** 22-33.

CHAERLE, L., HAGENBEEK, D., VANROBAEYS, X. & VAN DER STRAETEN, D. (2007) Early detection of nutrient and biotic stress in Phaseolus vulgaris. *International Journal of Remote Sensing,* **28,** 3479-3492.

CHANG, C.-I. & LIU, K.-H. (2014) Progressive band selection of spectral unmixing for hyperspectral imagery. *Ieee Transactions on Geoscience and Remote Sensing,* **52,** 2002-2017.

CHANG, C. I., DU, Q., SUN, T. L. & ALTHOUSE, M. L. G. (1999) A joint band prioritization and band-decorrelation approach to band selection for hyperspectral image classification. *Ieee Transactions on Geoscience and Remote Sensing,* **37,** 2631-2641.

CHANG, Y. C. & REID, J. F. (1996) RGB calibration for color image analysis in machine vision. *Ieee Transactions on Image Processing,* **5,** 1414-1422.

CHAPPELLE, E. W., KIM, M. S. & MCMURTREY, J. E. (1992) Ration analysis of reflectance spectra (RARS)-An algorithm for the remote estimation concentration of chlorophyll-a, chlorophyll-b, and carotenoid soybean leaves. *Remote Sensing of Environment,* **39,** 239-247.

CHEN, D. Y., HUANG, J. F. & JACKSON, T. J. (2005) Vegetation water content estimation for corn and soybeans using spectral indices derived from MODIS near- and short-wave infrared bands. *Remote Sensing of Environment,* **98,** 225-236.

CHEN, Y. & BARAK, P. (1982) Iron nutrition of plant in calcareous soils. *Advances in Agronomy,* **35,** 217-240.

CHENG, K. S., YEH, H. C. & TSAI, C. H. (2000) An anisotropic spatial modeling approach for remote sensing image rectification. *Remote Sensing of Environment,* **73,** 46-54.

CHENG, Y.-B., ZARCO-TEJADA, P. J., RIANO, D., RUEDA, C. A. & USTIN, S. L. (2006) Estimating vegetation water content with hyperspectral data for different canopy scenarios: Relationships between AVIRIS and MODIS indexes. *Remote Sensing of Environment,* **105,** 354-366.

CHERNICK, M. R., MURTHY, V. K. & NEALY, C. D. (1988) Estimation of error rate for linear discriminant functions by resampling - non-Gaussian populations. *Computers & Mathematics with Applications,* **15,** 29-37.

COZZOLINO, D., CYNKAR, W., SHAH, N. & SMITH, P. (2011a) Quantitative analysis of minerals and electric conductivity of red grape homogenates by near infrared reflectance spectroscopy. *Computers and Electronics in Agriculture,* **77,** 81-85.

COZZOLINO, D., CYNKAR, W., SHAH, N. & SMITH, P. (2011b) Technical solutions for analysis of grape juice, must, and wine: the role of infrared spectroscopy and chemometrics. *Analytical and Bioanalytical Chemistry,* **401,** 1475-1484.

CRANE, J. H. (2013) DISEASES OF AVOCADO. (Eds. C. F. BALERD & I. MAGUIRE).

CURRAN, P. (2000) Introduction to environmental remote sensing (fourth edition). *Geography,* **85,** 376-376.

DE CASTRO, A.-I., JURADO-EXPOSITO, M., GOMEZ-CASERO, M.-T. & LOPEZ-GRANADOS, F. (2012) Applying neural networks to hyperspectral and multispectral field data for discrimination of cruciferous weeds in winter crops. *TheScientificWorldJournal,* **2012,** 630390-630390.

DE CASTRO, A. I., EHSANI, R., PLOETZ, R. C., CRANE, J. H. & BUCHANON, S. (2015) Detection of Laurel Wilt Disease in Avocado Using Low Altitude Aerial Imaging. *Plos One,* **10**.

DEMELASH, T. & GETACHEW, W. (2015) Evaluation of avocado root rot (Phytophthora cinnamomi Rands) control options in southwest Ethiopia. *Journal of Biology, Agriculture and Healthcare,* **5,** 10-13.

DOBROWSKI, S. Z., PUSHNIK, J. C., ZARCO-TEJADA, P. J. & USTIN, S. L. (2005) Simple reflectance indices track heat and water stress-induced changes in steady-state chlorophyll fluorescence at the canopy scale. *Remote Sensing of Environment,* **97,** 403-414.

DONG, C.-W., YE, Y., ZHANG, J.-Q., ZHU, H.-K. & LIU, F. (2014) Detection of Thrips Defect on Green-Peel Citrus Using Hyperspectral Imaging Technology Combining PCA and B-Spline Lighting Correction Method. *Journal of Integrative Agriculture,* **13,** 2229-2235.

DREADEN, T. J., SMITH, J. A. & MAYFIELD, A. E. (2008) Development of a real-time PCR assay for detection of the Raffaelea species causing Laurel wilt disease. *Phytopathology,* **98,** S48-S48.

EVANS, E. A. (2015) Sample avocado production costs and profitability analysis for Florida. Electronic data information source (EDIS) FE 837. Food and resource economics department, university of Florida, Gainesville, FL. (Ed. I. BERNAL LOZANO).

EVANS, E. A., CRANE, J., HODGES, A. & OSBORNE, J. L. (2010) Potential economic impact of laurel wilt disease on the Florida avocado industry. *Horttechnology,* **20,** 234-238.

EVANS, J. P., SCHEFFERS, B. R. & HESS, M. (2014) Effect of laurel wilt invasion on redbay populations in a maritime forest community. *Biological Invasions,* **16,** 1581-1588.

EVERETT, K. R., REES-GEORGE, J., PUSHPARAJAH, I. P. S., MANNING, M. A. & FULLERTON, R. A. (2011) Molecular Identification of Sphaceloma perseae (Avocado Scab) and its Absence in New Zealand. *Journal of Phytopathology,* **159,** 106-113.

FAN, G., ZHA, J., DU, R. & GAO, L. (2009) Determination of soluble solids and firmness of apples by Vis/NIR transmittance. *Journal of Food Engineering,* **93,** 416-420.

FENG, L., CHEN, S., FENG, B., HE, Y., LOU, B., FENG, L., CHEN, S. S., FENG, B., HE, Y. & LOU, B. G. (2012) Spectral detection on disease severity of soybean pod anthracnose. *Nongye Jixie Xuebao = Transactions of the Chinese Society for Agricultural Machinery,* **43,** 175-192.

FENG, L., FANG, H., ZHOU, W.-J., HUANG, M. & HE, Y. (2006) Nitrogen stress measurement of canola based on multi-spectral charged coupled device imaging sensor. *Guang pu xue yu guang pu fen xi = Guang pu,* **26,** 1749-1752.

FENG, W., YAO, X., ZHU, Y., TIAN, Y. C. & CAO, W. (2008) Monitoring leaf nitrogen status with hyperspectral reflectance in wheat. *European Journal of Agronomy,* **28,** 394-404.

FERWERDA, J. G., SKIDMORE, A. K. & MUTANGA, O. (2005) Nitrogen detection with hyperspectral normalized ratio indices across multiple plant species. *International Journal of Remote Sensing,* **26,** 4083-4095.

FOODY, G. M., MCCULLOCH, M. B. & YATES, W. B. (1995) Classification of remotely-sensed data by an artificial neural-network - issues related to training data characteristics. *Photogrammetric Engineering and Remote Sensing,* **61,** 391-401.

FRAEDRICH, S. W., HARRINGTON, T. C., RABAGLIA, R. J., ULYSHEN, M. D., MAYFIELD, A. E., III, HANULA, J. L., EICKWORT, J. M. & MILLER, D. R. (2008) A fungal symbiont of the redbay ambrosia beetle causes a lethal wilt in redbay and other Lauraceae in the southeastern United States. *Plant Disease,* **92,** 215-224.

FRANKE, J. & MENZ, G. (2007) Multi-temporal wheat disease detection by multi-spectral remote sensing. *Precision Agriculture,* **8,** 161-172.

FRIDGEN, J. L. & VARCO, J. J. (2004) Dependency of cotton leaf nitrogen, chlorophyll, and reflectance on nitrogen and potassium availability. *Agronomy Journal,* **96,** 63-69.

FRIEDL, M. A. & BRODLEY, C. E. (1997) Decision tree classification of land cover from remotely sensed data. *Remote Sensing of Environment,* **61,** 399-409.

FU, X., YING, Y., LU, H. & XU, H. (2007) Comparison of diffuse reflectance and transmission mode of visible-near infrared spectroscopy for detecting brown heart of pear. *Journal of Food Engineering,* **83,** 317-323.

FUTACH, S., WEINGARTEN, S. & IREY, M. (2009) Determining HLB Infection Levels using Multiple Survey Methods in Florida Citrus. Proc. Fla. State Hort.

GAMON, J. A. & SURFUS, J. S. (1999) Assessing leaf pigment content and activity with a reflectometer. *New Phytologist,* **143,** 105-117.

GAO, B. C. (1996) NDWI - A normalized difference water index for remote sensing of vegetation liquid water from space. *Remote Sensing of Environment,* **58,** 257-266.

GARRETT, K. A., DENDY, S. P., FRANK, E. E., ROUSE, M. N. & TRAVERS, S. E. (2006) Climate change effects on plant disease: Genomes to ecosystems. *Annual Review of Phytopathology,* **44,** 489-509.

GENC, L., NALPULAT, M., KIZIL, U., MIRIK, M., SMITH, S. E. & MENDES, M. (2013) Determination of water stress with spectral reflectance on sweet corn (Zea mays L.) using classification tree (CT) analysis. *Zemdirbyste-Agriculture,* **100,** 81-90.

GILABERT, M. A., GONZALEZ-PIQUERAS, J., GARCIA-HARO, F. J. & MELIA, J. (2002) A generalized soil-adjusted vegetation index. *Remote Sensing of Environment,* **82,** 303-310.

GITELSON, A. A., GRITZ, Y. & MERZLYAK, M. N. (2003) Relationships between leaf chlorophyll content and spectral reflectance and algorithms for non-destructive chlorophyll assessment in higher plant leaves. *Journal of Plant Physiology,* **160,** 271-282.

GITELSON, A. A. & MERZLYAK, M. N. (1996) Signature analysis of leaf reflectance spectra: Algorithm development for remote sensing of chlorophyll. *Journal of Plant Physiology,* **148,** 494-500.

GOEL, P. K., PRASHER, S. O., LANDRY, J. A., PATEL, R. M., BONNELL, R. B., VIAU, A. A. & MILLER, J. A. (2003) Potential of airborne hyperspectral remote sensing to detect nitrogen deficiency and weed infestation in corn. *Computers and Electronics in Agriculture,* **38,** 99-124.

GOETZ, A. F. H., ROCK, B. N. & ROWAN, L. C. (1983) Remote-sensing for exploration-An overview. *Economic Geology,* **78,** 573-590.

GRAEFF, S. & CLAUPEIN, W. (2003) Quantifying nitrogen status of corn (Zea mays L.) in the field by reflectance measurements. *European Journal of Agronomy,* **19,** 611-618.

GREEN, M. J., THOMPSON, D. A. & MACKENZIE, D. J. (1999) Easy and efficient DNA extraction from woody plants for the detection of phytoplasmas by polymerase chain reaction. *Plant Disease,* **83,** 482-485.

GUNKEL, G., KOSMOL, J., SOBRAL, M., ROHN, H., MONTENEGRO, S. & AURELIANO, J. (2007) Sugar cane industry as a source of water pollution - case study on the situation in Ipojuca river, Pernambuco, Brazil. *Water Air and Soil Pollution,* **180,** 261-269.

HAAS, A. R. C. (1939) Avocado leaf symptoms characteristic of potassium, phosphate, manganese, and boron deficiencies in solution cultures. *Yearbook. California Avocado Society,* 103-109.

HABOUDANE, D., MILLER, J. R., PATTEY, E., ZARCO-TEJADA, P. J. & STRACHAN, I. B. (2004) Hyperspectral vegetation indices and novel algorithms for predicting green LAI of crop canopies: Modeling and validation in the context of precision agriculture. *Remote Sensing of Environment,* **90,** 337-352.

HABOUDANE, D., MILLER, J. R., TREMBLAY, N., ZARCO-TEJADA, P. J. & DEXTRAZE, L. (2002) Integrated narrow-band vegetation indices for prediction of crop chlorophyll content for application to precision agriculture. *Remote Sensing of Environment,* **81,** 416-426.

HAMED HAMID, M. (2005) Hyperspectral crop reflectance data for characterising and estimating fungal disease severity in wheat. *Biosystems Engineering,* **91,** 9-20.

HAMMOND, C. M., LUSCHEI, E. C., BOERBOOM, C. M. & NOWAK, P. J. (2006) Adoption of integrated pest management tactics by Wisconsin farmers. *Weed Technology,* **20,** 756-767.

HANULA, J. L., MAYFIELD, A. E., III, FRAEDRICH, S. W. & RABAGLIA, R. J. (2008) Biology and host associations of redbay ambrosia beetle (Coleoptera : Curculionidae : Scolytinae), exotic vector of laurel wilt killing redbay trees in the southeastern United States. *Journal of Economic Entomology,* **101,** 1276-1286.

HEERMANN, P. D. & KHAZENIE, N. (1992) Classification of multispectral remote-sensing data using a back-propagation neural network. *Ieee Transactions on Geoscience and Remote Sensing,* **30,** 81-88.

HENSON, J. M. & FRENCH, R. (1993) The polymerase chain reaction and plant disease diagnosis. *Annual Review of Phytopathology,* **31,** 81-109.

HOLBEN, B. N. (1986) Characteristics of maximum-value composite images from temporal AVHRR data *International Journal of Remote Sensing,* **7,** 1417-1434.

HORLER, D. N. H., DOCKRAY, M. & BARBER, J. (1983) The red edge of plant leaf reflectance. *International Journal of Remote Sensing,* **4,** 273-288.

HUANG, C. Y. L. & SCHULTE, E. E. (1985) Digestion of plant-tissue for analysis by ICP emission-spectroscopy. *Communications in Soil Science and Plant Analysis,* **16,** 943-958.

HUETE, A., JUSTICE, C. & LIU, H. (1994) DEVELOPMENT OF VEGETATION AND SOIL INDEXES FOR MODIS-EOS. *Remote Sensing of Environment,* **49,** 224-234.

INCH, S. A. & PLOETZ, R. C. (2012) Impact of laurel wilt, caused by Raffaelea lauricola, on xylem function in avocado, Persea americana. *Forest Pathology,* **42,** 239-245.

JACKSON, T. J., CHEN, D. Y., COSH, M., LI, F. Q., ANDERSON, M., WALTHALL, C., DORIASWAMY, P. & HUNT, E. R. (2004) Vegetation water content mapping using Landsat data derived normalized difference water index for corn and soybeans. *Remote Sensing of Environment,* **92,** 475-482.

JAYAWARDENA, A. W., FERNANDO, D. K. & ZHOU, M. C. (1997) Comparison of multilayer perceptron and radial basis function network as flood forecasting. IHS.

JEYAPRAKASH, A., DAVISON, D. A. & SCHUBERT, T. S. (2014) Molecular detection of the laurel wilt fungus, R*affaelea lauricola*. *Plant Disease,* **98,** 559-564.

JONES, J. B., JR. (2012) Plant nutrition and soil fertility manual. *Plant nutrition and soil fertility manual,* 304 pp.-304 pp.

KARIMI, Y., PRASHER, S. O., MCNAIRN, H., BONNELL, R. B., DUTILLEUL, P. & GOEL, P. K. (2005) Discriminant analysis of hyperspectral data for assessing water and nitrogen stresses in corn. *Transactions of the Asae,* **48,** 805-813.

KENDRA, P. E., MONTGOMERY, W. S., NIOGRET, J. & EPSKY, N. D. (2013) An uncertain future for American Lauraceae: a lethal threat from redbay ambrosia beetle and laurel wilt disease (a review). *American Journal of Plant Sciences,* **4,** 727-738.

KENDRA, P. E., MONTGOMERY, W. S., NIOGRET, J., PRUETT, G. E., MAYFIELD, A. E., 3RD, MACKENZIE, M., DEYRUP, M. A., BAUCHAN, G. R., PLOETZ, R. C. & EPSKY, N. D. (2014) North American Lauraceae: Terpenoid emissions, relative attraction and boring preferences of redbay ambrosia beetle, Xyleborus glabratus (Coleoptera: Curculionidae: Scolytina. *PloS one,* **9,** e102086-e102086.

KERANEN, M., ARO, E.-M., TYYSTJARVI, E. & NEVALAINEN, O. (2003) Automatic plant identification with chlorophyll fluorescence fingerprinting. *Precision Agriculture,* **4,** 53-67.

KINARD, G. R., SCOTT, S. W. & BARNETT, O. W. (1996) Detection of apple chlorotic leaf spot and apple stem grooving viruses using RT-PCR. *Plant Disease,* **80,** 616-621.

KINGSBURY, N. (1999) Image processing with complex wavelets. *Philosophical Transactions of the Royal Society a-Mathematical Physical and Engineering Sciences,* **357,** 2543-2560.

KNIPLING, E. B. (1970) PHYSICAL AND PHYSIOLOGICAL BASIS FOR THE REFLECTANCE OF VISIBLE AND NEAR IR RADIATION FROM VEGETATION. *Remote Sensing of Environment,* **1,** 155-159.

KREZDORN, A. H. (1974) Influence of rootstock on cold hardiness of avocados. *Proceedings of the Florida State Horticultural Society,* **86,** 346-348.

KUFLIK, T., PERTOT, I., MOSKOVITCH, R., ZASSO, R., PELLEGRINI, E. & GESSLER, C. (2008) Optimization of Fire blight scouting with a decision support system based on infection risk. *Computers and Electronics in Agriculture,* **62,** 118-127.

KUHNS, E. H., MARTINI, X., TRIBUIANI, Y., COY, M., GIBBARD, C., PENA, J., HULCR, J. & STELINSKI, L. L. (2014) Eucalyptol is an attractant of the redbay ambrosia beetle, Xyleborus glabratus. *Journal of Chemical Ecology,* **40,** 355-362.

KUMAR, A., LEE, W. S., EHSANI, R. J., ALBRIGO, L. G., YANG, C. H. & MANGAN, R. L. (2012) Citrus greening disease detection using aerial hyperspectral and multispectral imaging techniques. *Journal of Applied Remote Sensing,* **6,** 063542-063542.

LEES, B. G. & RITMAN, K. (1991) Decision-tree and rule-induction approach to integration of remotely sensed and GIS data in mapping vegetation in disturbed or hilly environments. *Environmental Management,* **15,** 823-831.

LEWIS, M., JOOSTE, V. & DE GASPARIS, A. A. (2001) Discrimination of arid vegetation with airborne multispectral scanner hyperspectral imagery. *Ieee Transactions on Geoscience and Remote Sensing,* **39,** 1471-1479.

LI, S., QIU, J., YANG, X., LIU, H., WAN, D. & ZHU, Y. (2014) A novel approach to hyperspectral band selection based on spectral shape similarity analysis and fast branch and bound search. *Engineering Applications of Artificial Intelligence,* **27,** 241-250.

LINDERMAN, R. G., MOORE, L. W., BAKER, K. F. & COOKSEY, D. A. (1983) STRATEGIES FOR DETECTING AND CHARACTERIZING SYSTEMS FOR BIOLOGICAL-CONTROL OF SOILBORNE PLANT-PATHOGENS. *Plant Disease,* **67,** 1058-1064.

LIU, A., DENG, X., WANG, P., LI, X., LIU, A. Q., DENG, X. J., WANG, P. R. & LI, X. L. (2003) Near infrared reflectance spectroscopy technique and applications in agriculture. *Southwest China Journal of Agricultural Sciences,* **16,** 98-102.

LIU, S., TIAN, J., WANG, L., ZHANG, Y., QIN, X., LUO, Y., ASIRI, A. M., AL-YOUBI, A. O. & SUN, X. (2012) Hydrothermal Treatment of Grass: A Low-Cost, Green Route to Nitrogen-Doped, Carbon-Rich, Photoluminescent Polymer Nanodots as an Effective Fluorescent Sensing Platform for Label-Free Detection of Cu(II) Ions. *Advanced Materials,* **24,** 2037-2041.

LUKINA, E. V., STONE, M. L. & RANN, W. R. (1999) Estimating vegetation coverage in wheat using digital images. *Journal of Plant Nutrition,* **22,** 341-350.

MA, R., YANG, B., ZHANG, L. & LIU, Z. (2012) Design and implementation of a forest fire monitoring system using a miniature unmanned aerial vehicle. *Journal of Zhejiang A&F University,* **29,** 783-789.

MACHADO, M., COLLAZO, C., PENA, M., COTO, O. & LOPEZ, M. O. (2013) First report of root rot caused by Phytophthora nicotianae in avocado trees (Persea americana) in Cuba. *New Disease Reports,* **28,** 9-9.

MACKENZIE, D. J., MCLEAN, M. A., MUKERJI, S. & GREEN, M. (1997) Improved RNA extraction from woody plants for the detection of viral pathogens by reverse transcription-polymerase chain reaction. *Plant Disease,* **81,** 222-226.

MAGWAZA, L. S., OPARA, U. L., NIEUWOUDT, H., CRONJE, P. J. R., SAEYS, W. & NICOLAI, B. (2012) NIR Spectroscopy Applications for Internal and External Quality Analysis of Citrus Fruit-A Review. *Food and Bioprocess Technology,* **5,** 425-444.

MAHLEIN, A. K., STEINER, U., DEHNE, H. W. & OERKE, E. C. (2010) Spectral signatures of sugar beet leaves for the detection and differentiation of diseases. *Precision Agriculture,* **11,** 413-431.

MARIOTTI, M., ERCOLI, L. & MASONI, A. (1996) Spectral properties of iron-deficient corn and sunflower leaves. *Remote Sensing of Environment,* **58,** 282-288.

MATTHEWS, G. A. (1996) The importance of scouting in cotton IPM. *Crop Protection,* **15,** 369-374.

MAYFIELD, A. E., III, BARNARD, E. L., SMITH, J. A., BERNICK, S. C., EICKWORT, J. M. & DREADEN, T. J. (2008a) Effect of propiconazole on laurel wilt disease development in redbay trees and on the pathogen in vitro. *Arboriculture & Urban Forestry,* **34,** 317-324.

MAYFIELD, A. E., III, PENA, J. E., CRANE, J. H., SMITH, J. A., BRANCH, C. L., OTTOSON, E. D. & HUGHES, M. (2008b) Ability of the redbay ambrosia beetle (Coleoptera : Curculionidae : Scolytinae) to bore into young avocado (Lauraceae) plants and transmit the laurel wilt pathogen (Raffaelea sp.). *Florida Entomologist,* **91,** 485-487.

MAYFIELD, A. E., III, SMITH, J. A., HUGHES, M. & DREADEN, T. J. (2008c) First report of Laurel wilt disease caused by a Raffaelea sp on avocado in Florida. *Plant Disease,* **92,** 976-976.

MCIVER, D. K. & FRIEDL, M. A. (2002) Using prior probabilities in decision-tree classification of remotely sensed data. *Remote Sensing of Environment,* **81,** 253-261.

MCMILLAN, J. (1976) DISEASES OF AVOCADO.

MENESATTI, P., ANTONUCCI, F., PALLOTTINO, F., ROCCUZZO, G., ALLEGRA, M., STAGNO, F. & INTRIGLIOLO, F. (2010) Estimation of plant nutritional status by Vis-NIR spectrophotometric analysis on orange leaves Citrus sinensis (L) Osbeck cv Tarocco. *Biosystems Engineering,* **105,** 448-454.

MERTON, R. & HUNTINGTON, J. (1999) Early simulation result of the ARIES-1 satellite sensor for multi-temporal vegetation research drived form AVIRIS., Pasadena, CA: NASA Jet Propulsion Lab. Available at ftp://popo.jpl.nasa.gov/pub/docs/workshop/99_docs/41.pdf.

MIN, M., LEE, W. S., KIM, Y. H. & BUCKLIN, R. A. (2006) Nondestructive detection of nitrogen in chinese cabbage leaves using VIS-NIR spectroscopy. *Hortscience,* **41,** 162-166.

MINSAVAGE, G. V., THOMPSON, C. M., HOPKINS, D. L., LEITE, R. & STALL, R. E. (1994) DEVELOPMENT OF A POLYMERASE CHAIN-REACTION PROTOCOL FOR DETECTION OF XYLELLA-FASTIDIOSA IN PLANT-TISSUE. *Phytopathology,* **84,** 456-461.

MIX, C., PICO, F. X. & OUBORG, N. J. (2003) A comparison of stereomicroscope and image analysis for quantifying fruit traits. *Seed Technology,* **25,** 12-19.

MORAN, M. S., INOUE, Y. & BARNES, E. M. (1997) Opportunities and limitations for image-based remote sensing in precision crop management. *Remote Sensing of Environment,* **61,** 319-346.

MOSHOU, D., BRAVO, C., OBERTI, R., WEST, J., BODRIA, L., MCCARTNEY, A. & RAMON, H. (2005) Plant disease detection based on data fusion of hyper-spectral and multi-spectral fluorescence imaging using Kohonen maps. *Real-Time Imaging,* **11,** 75-83.

MOSHOU, D., BRAVO, C., WAHLEN, S., WEST, J., MCCARTNEY, A., BAERDEMAEKER, J. D., RAMON, H. & DE BAERDEMAEKER, J. (2003) Simultaneous identification of plant stresses and diseases in arable crops based on a proximal sensing system and Self-Organising Neural Networks. *Precision agriculture: Papers from the 4th European Conference on Precision Agriculture, Berlin, Germany, 15-19 June 2003***,** 425-431.

MOSHOU, D., BRAVO, C., WEST, J., WAHLEN, T., MCCARTNEY, A. & RAMON, H. (2004) Automatic detection of 'yellow rust' in wheat using reflectance measurements and neural networks. *Computers and Electronics in Agriculture,* **44,** 173-188.

MUTANGAO, O. & KUMAR, L. (2007) Estimating and mapping grass phosphorus concentration in an African savanna using hyperspectral image data. *International Journal of Remote Sensing,* **28,** 4897-4911.

NASS/USDA (2009) Non-citrus fruits and nuts: 2008 preliminary summary FrNt1-3 (09) a. National Agricultral States Department of Agriculture, Washington, D.C.

NILSSON, H.-E. (1995) Remote sensing and image analysis in plant pathology. *Annual Review of Phytopathology,* **33,** 489-527.

NOH, H. & ZHANG, Q. (2012) Shadow effect on multi-spectral image for detection of nitrogen deficiency in corn. *Computers and Electronics in Agriculture,* **83,** 52-57.

NOH, H., ZHANG, Q., HAN, S., SHIN, B. & REUM, D. (2005) Dynamic calibration and image segmentation methods for multispectral imaging crop nitrogen deficiency sensors. *Transactions of the Asae,* **48,** 393-401.

OKAMOTO, H. & LEE, W. S. (2009) Green citrus detection using hyperspectral imaging. *Computers and Electronics in Agriculture,* **66,** 201-208.

OSBORNE, S. L., SCHEPERS, J. S., FRANCIS, D. D. & SCHLEMMER, M. R. (2002a) Detection of phosphorus and nitrogen deficiencies in corn using spectral radiance measurements. *Agronomy Journal,* **94,** 1215-1221.

OSBORNE, S. L., SCHEPERS, J. S., FRANCIS, D. D. & SCHLEMMER, M. R. (2002b) Use of spectral radiance to estimate in-season biomass and grain yield in nitrogen- and water-stressed corn. *Crop Science,* **42,** 165-171.

OSBORNE, S. L., SCHEPERS, J. S. & SCHLEMMER, M. R. (2004) Detecting nitrogen and phosphorus stress in corn using multi-spectral imagery. *Communications in Soil Science and Plant Analysis,* **35,** 505-516.

PAL, M. & MATHER, P. M. (2003) An assessment of the effectiveness of decision tree methods for land cover classification. *Remote Sensing of Environment,* **86,** 554-565.

PANT, P., HEIKKINEN, V., KORPELA, I., HAUTA-KASARI, M. & TOKOLA, T. (2014) Logistic regression-based spectral band selection for tree species classification: effects of spatial scale and balance in training samples. *Ieee Geoscience and Remote Sensing Letters,* **11,** 1604-1608.

PARK, J. & SANDBERG, I. W. (1993) Approximation and radial-basis-function networks. *Neural Computation,* **5,** 305-316.

PATTEY, E., STRACHAN, I. B., BOISVERT, J. B., DESJARDINS, R. L. & MCLAUGHLIN, N. B. (2001) Detecting effects of nitrogen rate and weather on corn growth using micrometeorological and hyperspectral reflectance measurements. *Agricultural and Forest Meteorology,* **108,** 85-99.

PENUELAS, J., BARET, F. & FILELLA, I. (1995) SEMIEMPIRICAL INDEXES TO ASSESS CAROTENOIDS CHLOROPHYLL-A RATIO FROM LEAF SPECTRAL REFLECTANCE. *Photosynthetica,* **31,** 221-230.

PENUELAS, J. & FILELLA, I. (1998) Visible and near-infrared reflectance techniques for diagnosing plant physiological status. *Trends in Plant Science,* **3,** 151-156.

PERNEZNY, K. & RAID, R. N. (2001) Occurrence of Bacterial Leaf Spot of Escarole Caused by Pseudomonas cichorii in the Everglades Agricultural Area of Southern Florida. *Plant Disease,* **85**.

PINTER, P. J., HATFIELD, J. L., SCHEPERS, J. S., BARNES, E. M., MORAN, M. S., DAUGHTRY, C. S. T. & UPCHURCH, D. R. (2003) Remote sensing for crop management. *Photogrammetric Engineering and Remote Sensing,* **69,** 647-664.

PLOETZ, R., SCHAFFER, B., VARGAS, A., KONKOL, J., SALVATIERRA, J., INCH, S., CAMPBELL, A. & WIDEMAN, R. (2013) Physiological impacts of laurel wilt on avocado. *Phytopathology,* **103,** 114-114.

PLOETZ, R. C., INCH, S. A., MARTINEZ, J. M. P. & WHITE, T. L., JR. (2012a) Systemic infection of avocado, Persia Americana, by *Raffaelea lauricola,* does not progress into fruit pulp or seed. *Journal of Phytopathology,* **160,** 491-495.

PLOETZ, R. C., PEREZ-MARTINEZ, J. M., SMITH, J. A., HUGHES, M., DREADEN, T., BLANCHETTE, R., HELD, B. & INCH, S. A. (2010) Laurel Wilt: a dangerous new disease of avocado in the Western Hemisphere. *Caribbean Food Crops Society 46th Annual Meeting and T-Star Invasive Symposium, July 11-17, 2010, Boca Chica, Dominican Republic***,** 97-106.

PLOETZ, R. C., PEREZ-MARTINEZ, J. M., SMITH, J. A., HUGHES, M., DREADEN, T. J., INCH, S. A. & FU, Y. (2012b) Responses of avocado to laurel wilt, caused by Raffaelea lauricola. *Plant Pathology,* **61,** 801-808.

POHL, C. & VAN GENDEREN, J. L. (1998) Multisensor image fusion in remote sensing: concepts, methods and applications. *International Journal of Remote Sensing,* **19,** 823-854.

PRABHAKAR, M., PRASAD, Y. G., THIRUPATHI, M., SREEDEVI, G., DHARAJOTHI, B. & VENKATESWARLU, B. (2011) Use of ground based hyperspectral remote sensing for detection of stress in cotton caused by leafhopper (Hemiptera: Cicadellidae). *Computers and Electronics in Agriculture,* **79,** 189-198.

PYDIPATI, R., BURKS, T. F. & LEE, W. S. (2006) Identification of citrus disease using color texture features and discriminant analysis. *Computers and Electronics in Agriculture,* **52,** 49-59.

QI, J., CHEHBOUNI, A., HUETE, A. R., KERR, Y. H. & SOROOSHIAN, S. (1994) A modified soil adjusted vegetation index. *Remote Sensing of Environment,* **48,** 119-126.

QIN, J., BURKS, T. F., RITENOUR, M. A. & BONN, W. G. (2009) Detection of citrus canker using hyperspectral reflectance imaging with spectral information divergence. *Journal of Food Engineering,* **93,** 183-191.

QIN, Z. H. & ZHANG, M. H. (2005) Detection of rice sheath blight for in-season disease management using multispectral remote sensing. *International Journal of Applied Earth Observation and Geoinformation,* **7,** 115-128.

RABAGLIA, R. J., DOLE, S. A. & COGNAT, A. I. (2006) Review of American Xyleborina (Coleoptera : Curculionidae : Scolytinae) occurring North of Mexico, with an illustrated key. *Annals of the Entomological Society of America,* **99,** 1034-1056.

REYNIERS, M. & VRINDTS, E. (2006) Measuring wheat nitrogen status from space and ground-based platform. *International Journal of Remote Sensing,* **27,** 549-567.

RODRIGUEZ, D., FITZGERALD, G. J., BELFORD, R. & CHRISTENSEN, L. K. (2006) Detection of nitrogen deficiency in wheat from spectral reflectance indices and basic crop eco-physiological concepts. *Australian Journal of Agricultural Research,* **57,** 781-789.

ROUJEAN, J. L. & BREON, F. M. (1995) ESTIMATING PAR ABSORBED BY VEGETATION FROM BIDIRECTIONAL REFLECTANCE MEASUREMENTS. *Remote Sensing of Environment,* **51,** 375-384.

ROUSE, J. W., HASS, R. H., SCHELL, J. A. & DEERING, D. W. (1973) Monitering vegetation system in the great plain with ERTS. Third symposium, NASA.

SANKARAN, S. & EHSANI, R. (2012) Detection of huanglongbing disease in citrus using fluorescence spectroscopy. *Transactions of the Asabe,* **55,** 313-320.

SANKARAN, S., EHSANI, R. & ETXEBERRIA, E. (2010a) Mid-infrared spectroscopy for detection of Huanglongbing (greening) in citrus leaves. *Talanta,* **83,** 574-581.

SANKARAN, S., EHSANI, R., INCH, S. A. & PLOETZ, R. C. (2012) Evaluation of visible-near infrared reflectance spectra of avocado leaves as a non-destructive sensing tool for detection of laurel wilt. *Plant Disease,* **96,** 1683-1689.

SANKARAN, S., MISHRA, A., EHSANI, R. & DAVIS, C. (2010b) A review of advanced techniques for detecting plant diseases. *Computers and Electronics in Agriculture,* **72,** 1-13.

SANKARAN, S., MISHRA, A., MAJA, J. M. & EHSANI, R. (2011) Visible-near infrared spectroscopy for detection of Huanglongbing in citrus orchards. *Computers and Electronics in Agriculture,* **77,** 127-134.

SCHLEMMER, M. R., FRANCIS, D. D., SHANAHAN, J. F. & SCHEPERS, J. S. (2005) Remotely measuring chlorophyll content in corn leaves with differing nitrogen levels and relative water content. *Agronomy Journal,* **97,** 106-112.

SCHNEIDER, W. L., SHERMAN, D. J., STONE, A. L., DAMSTEEGT, V. D. & FREDERICK, R. D. (2004) Specific detection and quantification of Plum pox virus by real-time fluorescent reverse transcription-PCR. *Journal of Virological Methods,* **120,** 97-105.

SCHOTT, J. R., SALVAGGIO, C. & VOLCHOK, W. J. (1988) RADIOMETRIC SCENE NORMALIZATION USING PSEUDOINVARIANT FEATURES. *Remote Sensing of Environment,* **26,** 1-&.

SERPICO, S. B., BRUZZONE, L. & ROLI, F. (1996) An experimental comparison of neural and statistical non-parametric algorithms for supervised classification of remote-sensing images. *Pattern Recognition Letters,* **17,** 1331-1341.

SERRANO, L., FILELLA, I. & PENUELAS, J. (2000) Remote sensing of biomass and yield of winter wheat under different nitrogen supplies. *Crop Science,* **40,** 723-731.

SIMS, D. A. & GAMON, J. A. (2002) Relationships between leaf pigment content and spectral reflectance across a wide range of species, leaf structures and developmental stages. *Remote Sensing of Environment,* **81,** 337-354.

SIMS, D. A. & GAMON, J. A. (2003) Estimation of vegetation water content and photosynthetic tissue area from spectral reflectance: a comparison of indices based on liquid water and chlorophyll absorption features. *Remote Sensing of Environment,* **84,** 526-537.

SINCLAIR, T. R., HOFFER, R. M. & SCHREIBER, M. M. (1971) Reflectance and internal structure of leaves from several crops during a growing season. *Agronomy Journal,* **63,** 864-868.

SIRISOMBOON, P., HASHIMOTO, Y. & TANAKA, M. (2009) Study on non-destructive evaluation methods for defect pods for green soybean processing by near-infrared spectroscopy. *Journal of Food Engineering,* **93,** 502-512.

STEVENS, H. E. (1922) Avocado diseases. *Florida Agric. Exper. Stat.***,** 23 pp.-23 pp.

STRACHAN, I. B., PATTEY, E. & BOISVERT, J. B. (2002) Impact of nitrogen and environmental conditions on corn as detected by hyperspectral reflectance. *Remote Sensing of Environment,* **80,** 213-224.

TARPLEY, L., REDDY, K. R. & SASSENRATH-COLE, G. F. (2000) Reflectance indices with precision and accuracy in predicting cotton leaf nitrogen concentration. *Crop Science,* **40,** 1814-1819.

THENKABAIL, P. S., ENCLONA, E. A., ASHTON, M. S. & VAN DER MEER, B. (2004) Accuracy assessments of hyperspectral waveband performance for vegetation analysis applications. *Remote Sensing of Environment,* **91,** 354-376.

THENKABAIL, P. S., GAMAGE, M. S. D. N. & SMAKHTIN, V. U. (2005) The use of remote sensing data for drought assessment and monitoring in Southwest Asia. *Research Report - International Water Management Institute***,** v + 25 pp.-v + 25 pp.

THENKABAIL, P. S., SMITH, R. B. & DE PAUW, E. (2000) Hyperspectral vegetation indices and their relationships with agricultural crop characteristics. *Remote Sensing of Environment,* **71,** 158-182.

THOMASSON, J. A., SUI, R., COX, M. S. & AL-RAJEHY, A. (2001) Soil reflectance sensing for determining soil properties in precision agriculture. *Transactions of the Asae,* **44,** 1445-1453.

TOMKIEWICZ, D. & PISKIER, T. (2012) A plant based sensing method for nutrition stress monitoring. *Precision Agriculture,* **13,** 370-383.

TUCKER, C. J. (1979) RED AND PHOTOGRAPHIC INFRARED LINEAR COMBINATIONS FOR MONITORING VEGETATION. *Remote Sensing of Environment,* **8,** 127-150.

TZENG, Y. C., CHEN, K. S., KAO, W. L. & FUNG, A. K. (1994) A dynamic learning neural-network for remote-sensing applications. *Ieee Transactions on Geoscience and Remote Sensing,* **32,** 1096-1102.

ULISSI, V., ANTONUCCI, F., BENINCASA, P., FARNESELLI, M., TOSTI, G., GUIDUCCI, M., TEI, F., COSTA, C., PALLOTTINO, F., PARI, L. & MENESATTI, P. (2011) Nitrogen concentration estimation in tomato leaves by VIS-NIR non-destructive spectroscopy. *Sensors,* **11,** 6411-6424.

VANWIE, P. & STEIN, M. (1977) LANDSAT DIGITAL IMAGE RECTIFICATION SYSTEM. *Ieee Transactions on Geoscience and Remote Sensing,* **15,** 130-137.

VILLASENOR, J. D., BELZER, B. & LIAO, J. (1995) WAVELET FILTER EVALUATION FOR IMAGE COMPRESSION. *Ieee Transactions on Image Processing,* **4,** 1053-1060.

VINA, A., GITELSON, A. A., RUNDQUIST, D. C., KEYDAN, G., LEAVITT, B. & SCHEPERS, J. (2004) Remote sensing - Monitoring maize (Zea mays L.) phenology with remote sensing. *Agronomy Journal,* **96,** 1139-1147.

VIOLA, P. & WELLS, W. M. (1997) Alignment by maximization of mutual information. *International Journal of Computer Vision,* **24,** 137-154.

VRINDTS, E., DE BAERDEMAEKER, J. & RAMON, H. (2002) Weed detection using canopy reflection. *Precision Agriculture,* **3,** 63-80.

WEST, J. S., BRAVO, C., OBERTI, R., LEMAIRE, D., MOSHOU, D. & MCCARTNEY, H. A. (2003) The potential of optical canopy measurement for targeted control of field crop diseases. *Annual Review of Phytopathology,* **41,** 593-614.

WIWART, M., FORDONSKI, G., ZUK-GOLASZEWSKA, K. & SUCHOWILSKA, E. (2009) Early diagnostics of macronutrient deficiencies in three legume species by color image analysis. *Computers and Electronics in Agriculture,* **65,** 125-132.

WU, D., FENG, L., ZHANG, C. & HE, Y. (2008) Early detection of Botrytis cinerea on eggplant leaves based on visible and near-infrared spectroscopy. *Transactions of the Asabe,* **51,** 1133-1139.

YAMAGUCHI, I., KATO, J., OHTA, S. & MIZUNO, J. (2001) Image formation in phase-shifting digital holography and applications to microscopy. *Applied Optics,* **40,** 6177-6186.

ZARCO-TEJADA, P. J., BERJON, A., LOPEZ-LOZANO, R., MILLER, J. R., MARTIN, P., CACHORRO, V., GONZALEZ, M. R. & DE FRUTOS, A. (2005) Assessing vineyard condition with hyperspectral indices: Leaf and canopy reflectance simulation in a row-structured discontinuous canopy. *Remote Sensing of Environment,* **99,** 271-287.

ZARCO-TEJADA, P. J., MILLER, J. R., MOHAMMED, G. H. & NOLAND, T. L. (2000) Chlorophyll fluorescence effects on vegetation apparent reflectance: I. Leaf-level measurements and model simulation. *Remote Sensing of Environment,* **74,** 582-595.

ZENTMYER, G. A. (1952) Collecting avocados in Central America for disease resistance tests. *Yearbook. California Avocado Society, 1952***,** 107-111.

ZENTMYER, G. A. (1984) AVOCADO DISEASES. *Tropical Pest Management,* **30,** 388-400.

ZHANG, Y., CONG, Q., XIE, Y., ZHAO, B., ZHANG, Y., CONG, Q., XIE, Y. F. & ZHAO, B. (2007) Progress in application of near infrared spectroscopy technology in agriculture. *Transactions of the Chinese Society of Agricultural Engineering,* **23,** 285-290.

ZHAO, D. L., REDDY, K. R., KAKANI, V. G., READ, J. J. & CARTER, G. A. (2003) Corn (Zea mays L.) growth, leaf pigment concentration, photosynthesis and leaf hyperspectral reflectance properties as affected by nitrogen supply. *Plant and Soil,* **257,** 205-217.

ZHAO, D. L., REDDY, K. R., KAKANI, V. G. & REDDY, V. R. (2005) Nitrogen deficiency effects on plant growth, leaf photosynthesis, and hyperspectral reflectance properties of sorghum. *European Journal of Agronomy,* **22,** 391-403.

ZIVKOVIC, Z. & VAN DER HEIJDEN, F. (2006) Efficient adaptive density estimation per image pixel for the task of background subtraction. *Pattern Recognition Letters,* **27,** 773-780.

ZYGIELBAUM, A. I., ARKEBAUER, T. J., WALTER-SHEA, E. A. & SCOBY, D. L. (2012) Detection and measurement of vegetation photoprotection stress response using PAR reflectance. *Israel Journal of Plant Sciences,* **60,** 37-47.

BIOGRAPHICAL SKETCH

Jaafar Jabbar Abdulridha was born in Babylon city south of Baghdad - Iraq in 1969. Bachelor's and M.S. degrees was earned from the Department of Agricultural Machinery at the University of Baghdad, in 1993 and 2002, respectively. The bachelor's degree was in general mechanization of agriculture. The master's degree was in sprinkler irrigation equipment system. In 2011, he got a scholarship from the University of Florida supported by Iraqi minister of higher education and science research. The major of his Ph.D. program is agricultural and biological engineering.